Enzymatic Biofuel Cells for Implantable and Microscale Devices

Scott Calabrese Barton,*,† Josh Gallaway,† and Plamen Atanassov‡

Department of Chemical Engineering, Columbia University, New York, New York 10027, and Department of Chemical and Nuclear Engineering, University of New Mexico, Albuquerque, New Mexico 87131

Received July 26, 2004

Contents

1. Introduction

Biological fuel cells have a long history in the literature,[1−3] but in recent years, they have come to prominence as more conventional fuel cell technologies have approached mass-market acceptance. Driving the recent ascendance of biofuel cells are the aspects of biocatalysis that are unmatched by conventional low-temperature oxidation−reduction catalysts, namely, activity at near-room temperatures and neutral pH and, more importantly, selective catalytic activity.

Although, until recently, the development of biofuel cell devices has not been extensive, research in biocatalytically modified electrodes, particularly for sensor applications, has provided substantial technological underpinning for current biofuel cell development. There exists significant overlap in technical requirements between sensors and biofuel cells, including chemical and mechanical stability, selectivity, and cost of materials. However, these two technologies diverge in the area of energy supply, in that sensors are generally energy-consuming cells and biofuel cells must, by definition, be energy producers. This significant difference leads to differing technical requirements, primarily in the areas of current density and cell potential. First, as a driven cell, sensors generally operate at cell potentials greater than open circuit. Second, cell current must be minimized to minimize power consumption. Generally, sensors are designed with currents in the nanoampere to microampere range such that power consumption is very small even for cell potentials near 1 V. Often, cell potential in a sensor must also be minimized to avoid undesired side reactions.

In contrast, as an energy-producing cell, an ideal enzymatic fuel cell generates maximum power, meaning both high current and high potential. Cell materials and structure must be designed such that overpotentials due to kinetics, ohmic resistance, and mass transfer are minimized and current density, particularly in terms of current per unit volume, is maximized. Although challenging in the context of biocatalyzed fuel cells, these issues are common to conventional fuel cell design. Indeed, since William Grove's original experiments in 1839, fuel cells have been stacked, i.e., arranged in series, to achieve higher total system voltage by multiplying individual cell voltage.[4]

A second issue that distinguishes biofuel cells from sensors is stability. Often, biocatalyzed electrochemical sensors are inexpensive enough to be disposable, and therefore, long-term stability is not essential. Should stability be required, one approach is to encapsulate the biocatalytic species in a low-porosity hydrophilic material, such as a silica gel.[5,6] Hydroxides on the gel surface interact with sugars of the enzyme shell to "cage" the enzyme, restricting translational motion and minimizing enzyme denaturation. Depending on the enzyme, caging of the molecule can result in reduced activity. Such gels also restrict the mobility of reactants and products, leading to mass-transfer limitations in the electrode. This might be a desired result in an amperometric sensor, where mass-transfer-limited signals are often linearly related to reactant concentration.

In contrast, stability is a key aspect of any practical fuel cell, and biofuel cells must have lifetimes ranging from months to years to justify implanted, highly distributed, or consumer portable applications. Such stability is often difficult to achieve in redox enzymes, although introduction of thermophilic species and the use of mutagenic techniques might provide future

* Corresponding author. E-mail: scb@cheme.columbia.edu.
† Columbia University.
‡ University of New Mexico.

10.1021/cr020719k CCC: $48.50
Published on Web 09/21/2004

Scott Calabrese Barton grew up in Jackson, MI, and earned a B.S. from the University of Notre Dame and a M.S. from the Massachusetts Institute of Technology, both in aerospace engineering. A stint as a noise control engineer at General Motors led to an interest in quiet, efficient electrochemical power, and he returned to earn a Ph.D. in chemical engineering from Columbia University (with Alan West). He was a postdoctoral associate at the University of Texas at Austin (with Adam Heller) and then returned to Columbia as Assistant Professor of Chemical Engineering in 2001. His research focuses on high-rate biocatalytic electrodes for low-temperature fuel cells.

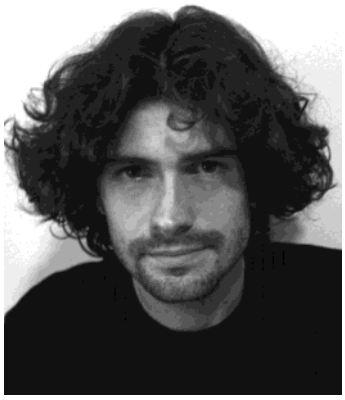

Josh Gallaway was born in Waverly, TN, in 1974 and lived there until attending Case Western Reserve University in 1992, where he earned a B.S. in chemical engineering. Since 2002, he has been a graduate student at Columbia University, studying redox polymer–enzyme systems for use in biofuel cells.

improvements.[7] The sol−gel caging techniques described above might be applicable to biocatalyzed fuel cell electrodes, but the effects of caging on enzyme activity and species transport are significant concerns. Moreover, supporting materials such as mediators and polymer gels are similarly susceptible to attack by ambient chemical species and mechanical stress imparted by convecting fluids.[8−10] Thus, although sensor designs can act as starting point for biofuel cell development, the demands of high power and stability ultimately lead the biofuel cell design process down an independent path.

Extensive review literature exists in the area of biological fuel cells. Notably, Palmore and Whitesides summarized biological fuel cell concepts and performance up to 1992.[11] More recently, Katz and Willner discussed recent progress in novel electrode chemistries for both microbial and enzymatic fuel cells,[12] and Heller reviewed advances in miniature cells.[13] This article does not duplicate these valuable contributions. Instead, we focus on the strengths and weaknesses of the technology in the context of specific classes of applications and point to areas where additional knowledge is required to properly exploit biological fuel cells. With some exceptions, we focus on contributions made after 1992.

Plamen Atanassov grew up in Bulgaria and graduated from the University of Sofia in 1987 specializing in Chemical Physics and Theoretical Chemistry. He joined the Bulgarian Academy of Sciences and become a Member of Technical Staff of its Central Laboratory of Electrochemical Power Sources. During 1988–1989, he was a visiting scientist in the Frumkin's Institute of Electrochemistry, Moscow, Russia, studying bioelectrochemistry of enzymes. He received his doctorate from the Bulgarian Academy of Sciences in Physical Chemistry/Electrochemistry under the guidance of Prof. Ilia Iliev. He moved to the United States in 1992 and later became a research faculty member at the University of New Mexico. In 1999, he joined Superior MicroPowders LLC (now Cabot-SMP), where he was a project leader in fuel cell electrocatalysts development. He returned to the University of New Mexico in 2000 as an Assistant Professor of Chemical and Nuclear Engineering. His research programs include development of non-platinum electrocatalyst for fuel cells, new materials and technologies for micro-power sources, enzymatic biofuel cells, sensor systems design, and integration of microanalytical systems.

Biofuel cells have traditionally been classified according to whether the catalytic enzymes were located inside or outside of living cells. If living cells are involved, the system is considered to be microbial, and if not, the system is considered enzymatic. Although microbial fuel cells exhibit unique features unmatched by enzymatic cells, such as long-term stability and fuel efficiency, the power densities associated with such devices are typically much lower owing to resistance to mass transfer across cell membranes. Thus, microbial fuel cells are expected to find limited application in small-scale electronic devices. This review focuses on enzymatic biofuel cells. Generally speaking, such cells demonstrate reduced stability because of the limited lifetime of extracellular enzymes and are unable to fully oxidize fuels, but they allow for substantial concentration of catalysts and removal of mass-transfer barriers. Enzymatic biofuel cells therefore produce higher current and power densities, approaching the range of applicability to micro- and miniscale electronics applications.

2. Applications

We begin with a discussion of key applications that can be addressed by biofuel cells and key requirements derived therefrom. The range of possible applications can be broken down into three main

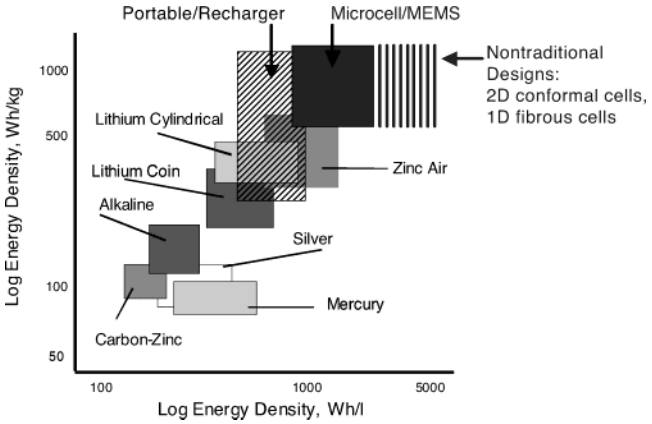

Figure 1. Conceptual product definitions of enzyme-based biofuel cells as they are compared in their specific energy and energy density to the existing primary battery technology. Based on Figure 2 of ref 15. Reproduced with permission. Copyright 1999 The Electrochemical Society, Inc.

subclasses: (1) implantable power, such as microscale cells implanted in human or animal tissue or larger cells implanted in blood vessels; (2) power derived from ambient fuels or oxidants, mainly plant saps or juices, but extendable to sewage and other waste streams; and (3) power derived from conventional fuels, including hydrogen, methanol, and higher alcohols.

Classes 1 and 2 are closely related: The reactants available for implantable power, such as blood-borne glucose, lactate, or oxygen, are ambient in that environment. These two classes are distinct, however, in that an ambient-fueled cell need not be implanted and utilizes plant- or waste-derived fuels, whereas the implantable cell utilizes animal-derived fuels. Class 3 is unique because it competes with well-established conventional fuel cell technology.

All three classes share the fundamental technical requirements of high power density and high stability. Identifying the required energy density and specific energies of biofuel cells depends on their potential product definitions. Microbial fuel cells serve in specific applications where size is not a limitation and the rate of current drain is small: marine power for stationary devices (buoys) or recharging devices based on biological hydrogen gas production.[14] Enzyme-based biofuel cells can be formatted into portable power sources (including portable rechargers) and micro-miniature power sources for independent power-on-chip or microelectromechanical (MEMS) based systems (see Figure 1). The large molecular size of biocatalysts enables implementation of bionanotechnologies in enzyme-based power sources. As a result, one can envision novel design concepts that can substantially deviate from existing power supply form factors: two-dimensional devices for conformal power sources (power-generating coatings) and one-dimensional, fibrous devices leading to "power textiles".

Figure 1 juxtaposes the energy fields of these three potential product definitions with that of conventional primary battery technology. The data on the energy densities for the battery product definitions were adopted from a recent technology review.[15] The expected energy performance figures for biofuel cells are based on data available in the literature in a variety of formats. It was found that, depending on key technology directions, for example, toward a portable, reserve power or microsystem power application, the results fall into two specific energy ranges. The "shift" toward higher volumetric energy densities in microcell MEMS-based technologies is due to advantages derived from the use of microfabrication techniques in layered structure formation and packaging. As in any fuel cell, critical advantage is derived from the fact that fuel is supplied to the cell, rather than being embedded within it.

2.1. Implantable Power

The most intuitive application of biofuel cells is for implantable power. Biocatalysts are physiological species and have evolved to function in complex physiological environments, efficiently catalyzing reactions at physiological temperature and pH, involving fuels and oxidants present in such environments, and for the most part producing reaction products that are tolerable to the host organism. The selectivity of enzymatic catalysts stands out under such conditions, because no separation of fuel and oxidant is required, as is the case with noble metal catalysts. Additionally, these species generally demonstrate peak activity at physiological temperatures (25−50 °C), and many species have high activity at near-neutral pH. Therefore, the biocatalytic electrodes need not be separated or sealed off from physiological fluids. This allows for simpler cell design and access to high mass-transfer rates because of the presence of ambient convection.

A number of implantable medical devices might benefit from implanted power supplies. The most obvious is the cardiac pacemaker, which has been in use for over 40 years and is currently powered by a lithium−iodine battery with an operating power output of ~1 μW and lifetimes exceeding 10 years.[16,17] The typical energy density of such a battery is 1 W·h/mL; a biofuel cell generating 10 mW/mL, on the high end of what is possible today, would generate equivalent energy in just 4 days. Indeed, the benefit of an implantable biofuel cell compared to a conventional battery is one of high power density and, in some sense, infinite energy density if energy can be derived from physiologically ambient sugars.

A growing field of "functional electrical stimulation" exists wherein artificially applied electrical current is used to control the nervous system, allowing limited control of leg, arm, and finger movement.[18−20] The power requirements of such systems greatly exceed that of pacemakers, and power for one such device, along with control signals, is provided by radio-frequency induction via a coil implanted in the patient's chest.[21] Implantable power supplies providing milliwatt-scale power would greatly simplify the design of such systems. Other prosthetic applications such as artificial hearing or vision might also benefit from such a device.[22−24]

Stability of implanted biofuel cells requires chemical stability in the presence of numerous physiologically active species that attack key electrode components. For example, electrodes exposed to physiological

fluids must be active and stable at neutral pH. This requirement eliminates the majority of fungal laccase species, which are capable of reducing oxygen at high potential but have peak activity in the pH 4−5 range and are essentially inactive at pH 7.[25,26] Constituent species of blood serum have also been shown to decrease stability of a redox polymer-mediated glucose oxidase electrode.[27] Oxidation products of serum-borne urate were found to precipitate in the enzyme-immobilizing hydrogel, interfering with electron transfer, although not inhibiting the activity of the enzyme itself. Zinc and iron cations, however, were shown to reduce both the intrinsic activity of glucose oxidase and the rate of electron transfer, the latter by cross-linking of the polymer gel. High-power devices will likely require ambient convection such as blood flow, raising the issue of mechanical stability as discussed above. Biological stability, associated with the natural immune response to foreign materials, has not yet received significant attention in the context of biofuel cells.

Some of these stability issues can be addressed by the use of protective barrier membranes,[28,29] at the risk of aggravating another fundamental challenge: reactant mass transfer. Typical reactants present in vivo are available only at low concentrations (glucose, 5 mM; oxygen, 0.1 mM; lactate, 1 mM). Maximum current density is therefore limited by the ability of such reactants to diffuse to and within bioelectrodes. In the case of glucose, flux to cylindrical electrodes embedded in the walls of blood vessels, where mass transfer is enhanced by blood flow of 1−10 cm/s, is expected to be 1−2 mA/cm^2.[30] Mass-transfer rates are even lower in tissues, where such convection is absent. However, microscale electrodes with fiber or microdot geometries benefit from cylindrical or spherical diffusion fields and can achieve current densities up to 1 mA/cm^2 at the expense of decreased electrode area.[31]

Finally, a complex issue associated with implantable devices is the implantation process itself, involving surgical procedures for inserting, electrically wiring, and stabilizing a device. A biofuel cell implanted in a blood vessel presents significant problems in that it must not act as a clotting agent, must not lead to substantial pressure drop, and must be electrically connected (wired) to the outside of the vessel so that the power produced is accessible. Above all, the host vessel walls must not be damaged by the insertion or ongoing presence of the cell. Indeed, a surgical procedure such as this is worthwhile only if the cell itself is stable and benign enough to last more than a year.

The surgical issues associated with tissue-implanted biofuel cells are less demanding, allowing practical short-term implantation with reduced stability requirements. However, material toxicity is an additional medical issue that does impact tissue-implanted cells. Enzymes such as glucose oxidase (EC 1.1.3.4), laccase (EC 1.10.3.2), and bilirubin oxidase (EC 1.3.3.5) have no known toxicity in the milligram quantities considered for implanted cells, and some synthetic species have received "Generally Recognized as Safe" (GRAS) status from the U.S. Food and Drug Administration (FDA).[32,33] Reaction products such as gluconolactone and peroxide are expected to be present in low concentrations.

However, some associated materials might be perceived as toxic. For example, complexes of osmium find frequent use as electron mediators, because of their rich chemistry, stability, and redox activity. Osmium metal and most compounds are considered nontoxic, but the neat tetroxide of osmium is a strong oxidizer and is considered "highly toxic" in the U.S. and "very toxic" by the European Union. On the other hand, the aqueous solution, osmic acid, has been injected at ∼1% concentration in several European clinical trials, starting in the 1970s, for treatment of arthritis and hemophilia.[34,35] No toxic effects were observed. Thus, osmium toxicity might be a question not of in vivo chemistry, but of manufacture, where a concentrated form of the oxide might need to be handled.[36]

2.2. Power from Ambient Fuels

The exploitation of ambient fuels is attractive in situations where power needs for small electronic devices are distributed, disconnected, and long-term. This might be true for electronic sensor systems for monitoring of plant health, air quality, weather, or the presence of biohazards. In principle, the fuel can be derived from carbohydrates contained in plants or from effluent of human or animal processes.

The monosaccharides glucose and fructose and the disaccharide sucrose, a glucose−fructose dimer, are the primary organic constituents of most plant saps. For example, sugar maple sap is composed of up to 5.4 wt % sucrose (150 mM), with less than 0.2% (11 mM) glucose.[37] In contrast, apple juice is typically 12 wt % sugar with a 1:1:2 mass ratio of sucrose/glucose/fructose, and other juices vary in the relative content of these three sugars.[38−40] Oxidation biocatalysts with activity toward these species are well-known and include glucose oxidase (EC 1.1.3.4), glucose dehydrogenase (EC 1.1.99.17),[41] pyranose oxidase (EC 1.1.3.10),[42] and oligosaccharide dehydrogenase.[43−46] Of these, the most active is glucose oxidase, and the most active substrate (reactant species) is glucose.

The issues associated with ambient fuel cells are similar to the implantable issues except that the cell itself need not be implanted and immunoreponse is not as severe. However, utilization of some sugars, such as fructose and sucrose, is not straightforward using well-characterized enzyme systems. This presents a challenge to the utilization of high-fructose and -sucrose species such as maple trees. There are opportunities to "bioreform" such sugars to glucose using enzymes such as invertase (aka sucrase, EC 3.2.1.26).[47]

2.3. Conventional Fuel Cells

Conventional fuel cell systems provide the designer with greater control over operating conditions as compared to the implantable and ambient-fuel categories. For example, the pH of the system can be adjusted well above or below neutral, and the opportunity exists to eradicate all poison species from the system. As previously mentioned, the realm of

conventional fuel cells is crowded with a variety of well-understood technologies that delivers high performance with respect to power density and efficiency. For example, platinum-based hydrogen−air fuel cell electrodes typically operate near 1 A/cm^2 and 0.65 V, and methanol cells achieve 500 mA/cm^2 at 0.5 V, orders of magnitude higher than the 1−10 mA/cm^2 current densities obtainable using the best reported methanol−air biofuel cells to date.[48,49]

To compete in this arena, biofuel cells must take advantage of inherent biocatalytic properties that cannot be duplicated by conventional technology. Among these key properties are (1) activity at low temperature and near-neutral pH, (2) chemical selectivity, and (3) potentially low-cost production using fermentation and bioseparation technologies. To the extent possible, these properties must be exploited with minimal compromise of power density and stability. This constraint leaves one major class of conventional applications suitable for biofuel cells: small fuel cells for portable power.

Small, direct methanol fuel cells (DMFCs) provide several potential points of entry. First, the current densities of such systems are typically lower, on the order of 100−300 mA/cm^2, owing to the high kinetic resistance associated with methanol oxidation as compared to hydrogen oxidation. Second, significant material issues are associated with the use of methanol in such cells. One particular issue is methanol crossover. DMFC performance is limited by methanol permeation (crossover) from the anode to the cathode side through commonly used Nafion polymer electrolyte membranes. Methanol crossover reduces fuel efficiency, because the crossover fuel oxidizes catalytically with oxygen at the cathode and depolarizes the cell by lowering the cathode open-circuit potential.[50] Several approaches to this problem exist, each with its own flaws, but one relevant solution is the use of "selective" oxygen reduction electrocatalysts that do not catalyze the oxidation of methanol, enabling the use of conventional membranes and low temperatures. In the past 30 years, two major classes of transition metal compounds have been proposed as selective oxygen reduction catalysts: macrocyclic complexes such as porphyrins and phthalocyanins[51−53] and transition metal chalcogenides (e.g., $Mo_xRu_ySe_z$).[54,55] Although all of the mentioned catalysts ameliorate losses associated with methanol crossover, they are less active and typically less stable than platinum.

Lastly, cost is a crucial issue in the commercialization of fuel cells, particularly as performance and lifetimes have improved to the threshold of practicability. The major costs associated with these systems are materials-related, with separator and catalyst materials at the top of the list. It is envisioned that the cost of separator materials will decrease with increased production and competition and as alternative materials are perfected. However, the cost of conventional noble metal catalysts, particularly platinum, is expected only to increase with increased production and demand.[56] Therefore, the cost issue could perhaps be addressed by employing alternative catalysts, including biocatalysts. Enzymes are derived from natural sources and can be manufactured at very low cost using well-established fermentation techniques.

3. Microbial Biofuel Cells

Microbial biofuel cells were the earliest biofuel cell technology to be developed, as an alternative to conventional fuel cell technology. The concept and performance of several microbial biofuel cells have been summarized in recent review chapters.[11,12] The most fuel-efficient way of utilizing complex fuels, such as carbohydrates, is by using microbial biofuel cells where the oxidation process involves a cascade of enzyme-catalyzed reactions.[57] The two classical methods of operating the microbial fuel cells are (1) utilization of the electroactive metabolite produced by the fermentation of the fuel substrate[58−61] and (2) use of redox mediators to shuttle electrons from the metabolic pathway of the microorganism to the electrodes.[62−65]

Recently, a novel microbial fuel cell harvesting energy from the marine sediment−seawater interface has been reported.[14] Also, a novel photosynthetic biofuel cell that is a hybrid between a microbial and enzymatic biofuel cell has been reported for the very first time.[66] More recently, reports of an unconventional biomass-fueled ceramic fuel cell can also be found in the literature.[67] A new concept of "Gastrobots"—hybrid robots that utilize operational power derived from microbial fuel cells—has been introduced.[68] Finally, the generation of electrical power by direct oxidation of glucose was demonstrated in mediatorless microbial fuel cells, which produced currents up to 3 μA/cm^2 at unknown cell voltage.[69]

Microbial- and enzyme-based biofuel cells share the characteristic of integrated biocatalytic systems: active enzymes derived from living microorganisms. Technical issues, level of maturity, and practical limitations of the two subdivisions of this technology, however, vary considerably. The two avenues also differ in the level of achieved power densities, although direct comparison is difficult in light of the 10−1000 times smaller size of the enzymatic type. While progress in microbial fuel cell research is expected to continue, we focus our discussion in the following sections on the concepts, challenges, and recent developments in enzymatic biofuel cells.

4. Bioelectrochemistry at the Cathode and Anode of Enzymatic Biofuel Cells

Enzyme biocatalyst assemblies on electrode surfaces usually do not achieve significant electron-transfer communication between the redox center and the conductive support, mostly because of the electrical insulation of the biocatalytic site by the surrounding protein matrixes.[70] During the past four decades, several methods have been proposed and investigated in the field of bioelectrochemical technology in an effort to establish efficient electrical communication between biocatalysts and electrodes.[71−81] In general, electron transfer is classified by two different mechanisms (see Figure 2):

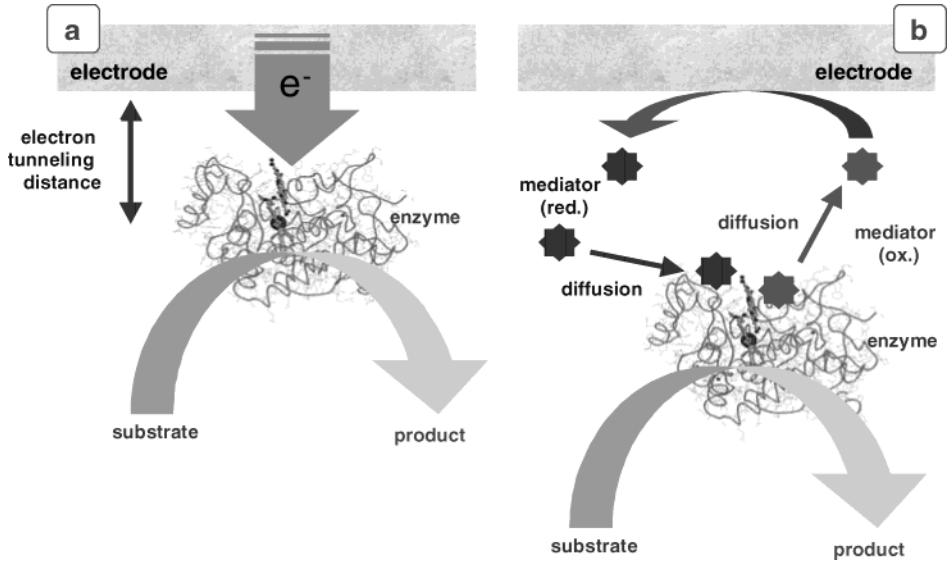

Figure 2. Alternative electron-transfer mechanisms. (a) Direct electron transfer (tunneling mechanism) from electrode surface to the active site of an enzyme. (b) Electron transfer via redox mediator.

mediated electron transfer (MET) and direct electron transfer (DET).

In MET, a low-molecular-weight, redox-active species, referred to as a mediator, is introduced to shuttle electrons between the enzyme active site and the electrode.[80] In this case, the enzyme catalyzes the oxidation or reduction of the redox mediator. The reverse transformation (regeneration) of the mediator occurs on the electrode surface. The major characteristics of mediator-assisted electron transfer are that (i) the mediator acts as a cosubstrate for the enzymatic reaction and (ii) the electrochemical transformation of the mediator on the electrode has to be reversible. In these systems, the catalytic process involves enzymatic transformations of both the first substrate (fuel or oxidant) and the second substrate (mediator). The mediator is regenerated at the electrode surface, preferably at low overvoltage. The enzymatic reaction and the electrode reaction can be considered as separate yet coupled.

Mediators can exist free in solution; physically entrapped behind a membrane;[82,83] immobilized in a matrix along with the biocatalyst;[84,85] or covalently bound to a surface or polymer network,[71] wherein the polymer can be conductive or insulating.[77,78] Detailed discussion of the various formats is outside scope of this review paper. However, selected immobilization chemistries reported in relation to enzymatic biofuel cells are reviewed in the sections below.

In DET, the enzymatic and electrode reactions are coupled by direct (mediatorless) electron transfer.[81] In this case, the electron is transferred directly from the electrode to the substrate molecule (or vice versa) via the active site of the enzyme. In such a system, the coupled overall process is the redox transformation of the substrate(s), which can be considered as an enzyme-catalyzed electrode process. According to this mechanism, the electrode surface acts as the enzyme cosubstrate, and the enzymatic and electrode reactions cannot be considered as separate, but as formal stages of the bioelectrocatalytic reaction mechanism. The catalytic effect of the enzyme is the reduction of the overvoltage for reaction of the substrate.

4.1. Enzyme-Catalyzed Direct Electron Transfer

The physicochemical manifestations of bioelectrocatalysis were the focus of intensive investigations during the 1980s. A number of enzymes were found to be capable of direct electron transfer with an electrode, including cytochrome *c*, peroxidase, ferredoxin, plastocyanin, azurin, azotoflavin, and glucose oxidase.[86−88] Studies of DET with these enzymes led to an electrochemical basis for the investigation of protein structure, mechanisms of redox transformations of protein molecules, and metabolic processes involving redox transformations. Depending on the practical significance of the substrates of these enzymatic reactions, electroanalytical applications of bioelectrocatalysis have begun to appear since the late 1980s.[43,79,89−91] Recently, the ability of oxidoreductase enzymes to catalyze direct electron transfer has been demonstrated for laccase, lactate dehydrogenase, peroxidase, hydrogenase, *p*-cresolmethylhydroxylase, methylamine dehydrogenase, succinate dehydrogenase, fumarate reductase, D-fructose dehydrogenase, alcohol dehydrogenase, and D-gluconate dehydrogenase.[79]

Application of these bioelectrocatalysts is based on their ability to interact with the electrode surface, forming a "molecular transducer" that converts a chemical signal directly into an electric one.[79] Among the oxidoreductases, of particular interest are those that catalyze either reduction of oxygen; oxidation of hydrogen, alcohols, and sugars; or transformation of peroxide. These common molecules are of importance for signal generation in biosensors and current generation in biofuel cells. Peroxidase is known to catalyze oxidation of a broad range of polyphenols and aromatic polyamines. Laccase, a copper-containing oxidase, exhibits substrate specificity similar to that of peroxidase.[92] Laccase catalyzes the oxidation of these substrates by molecular oxygen, forming

water. Peroxidase and laccase were early targets for the investigation of DET reactions.

Direct-electron-transfer (DET) characteristics of laccase on monolayer-modified gold electrodes were studied.[93] Three different monolayers were investigated, from which 4-aminothiophenol was found to be optimal for the direct electron transfer to take place. The electrocatalytic reduction of the oxygen at the electrode surface was very much dependent on the orientation of the enzyme and the method of immobilization. Fungal laccase from *Coriolus hirsutus* modified with sodium periodate demonstrated a higher anodic onset potential for oxygen reduction than the tree laccase from *Rhus vernicifera*. Physical immobilization of the enzyme did not give any shifts in anodic potential. A maximum anodic shift in reduction potential of 300 mV was observed for fungal laccase covalently coupled on the electrode surface.

4.2. Biomimetic Electrocatalysts for Fuel Cells

Investigations of enzyme-catalyzed direct electron transfer introduce the basis for a future generation of electrocatalysts based on enzyme mimics. This avenue could offer new methods of synthesis for nonprecious metal electrocatalysts, based on nanostructured (for example, sol−gel-derived) molecular imprints from a biological catalyst (enzyme) with pronounced and, in some cases, unique electrocatalytic properties. Computational approaches to the study of transition state stabilization by biocatalysts has led to the concept of "theozymes".[94]

Understanding the chemistry of the active site during the reaction process is the first step in electrode design and, ultimately, toward biomimetic catalysis. An example are laccases, which are glycosylated multicopper oxidases that oxidize a wide variety of substrates such as diphenols, aryldiamines, and aminophenols. Fungal laccases are less substrate specific than plant laccases.[95] Spectroscopic and X-ray crystallographic studies have revealed that they contain one blue copper or T1 site and a T2/T3 trinuclear copper cluster site (Figure 3). T2 is the normal copper, and T3 is a bridged copper pair. The cysteine bound to the T1 copper is flanked on either side by histidines that are ligated to each of the T3 coppers, providing a 1.3-nm pathway for electron transfer from the T1 to the trinuclear cluster.[96]

Electrons acquired by the T1 site from the oxidized cosubstrate are transferred internally by electron tunneling through the cystein−histidine pathway to the trinuclear site, where oxygen reduces to form water.[97] The four-electron reduction of dioxygen occurs in two two-electron steps. The fully reduced site first reacts with O_2 to generate a peroxide-level intermediate, which is then further reduced to a hydroxide product by uptake of electrons from T1 and T2, thus bridging the T2 and one of the T3 coppers in the trinuclear copper site. The first step, peroxide formation, is rate limiting, but the overall rate-limiting step is the oxidation of cosubstrate (or reduction of the T1 site), which is strictly outer sphere, involving no binding pocket.[92]

The redox potential of blue copper oxidases varies from species to species. The high redox potential of around 700 mV in fungal laccase is primarily attributed to nonaxial methionine ligand, a geometry that stabilizes the reduced state. Other factors such as solvent accessibility, dipole orientation, and hydrogen bonding also play an important role.[98,99]

Different chemical environments surrounding the T1 copper result in different redox potentials. Fungal laccases demonstrate the highest potential, close to the equilibrium potential of oxygen reduction in their respective pH regions (see Table 1). Laccases, however, are anion sensitive, with deactivation involving dissociation of T2 copper from the active site of the enzyme. Alternative copper oxidases such as bilirubin oxidase[100,101] and ceruloplasmin[102−105] also have high redox potentials, but their electrochemistry is less well understood and is still being explored.

4.3. Mediated Electron Transfer

The main purpose of redox mediation is to increase the rate of electron transfer between the active site of enzyme biocatalysts and an electrode by eliminating the need for the enzyme to interact directly with the electrode surface. Depending on the enzyme and

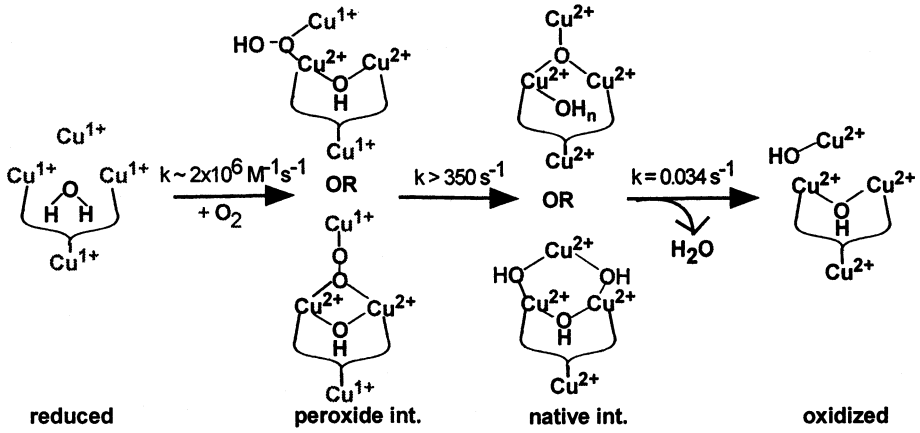

Figure 3. Molecular mechanism for the 4e⁻ reduction of O_2 to H_2O by the multicopper oxidases. Reprinted with permission from ref 99. Copyright 2001 American Chemical Society.

Table 1. Redox Potentials of T1 Copper Site in Some Copper-Containing Enzymes (E^0 in mV vs SHE) and the pH at Which It Was Estalished[92]

enzyme	E^0, mV (pH)	enzyme	E^0, mV (pH)
Laccases		Ascorbate Oxidase	
Polyporus versicolor	775−785 (pH 4.0)	*Cucurbita pepo medullosa*	344 (pH 7.4)
Polyporus pinsitus	760−790 (pH 4.0)	*Cucumis sativus*	350 (pH 7.4)
Coriolus hirsutus	750−850 (pH 4.0)		
Rhizoctonia solani	680−730 (pH 4.0)	Ceruloplasmin	
Trametes versicolor	780−800 (pH 4.0)	human I	490−580 (pH 7.4)
Pycnoporus cinnabarinus	740−760 (pH 7.0)	bovine	370−390 (pH 7.4)
Myrothecium verrucaria	480−490 (pH 7.4)		
Scytalidium thermophilum	480−530 (pH 7.0)	Bilirubin Oxidase	
Rhus Vernicifera	394−434 (pH 7.0)	*Myceliophthora thermophila*	450−480 (pH 7.0)

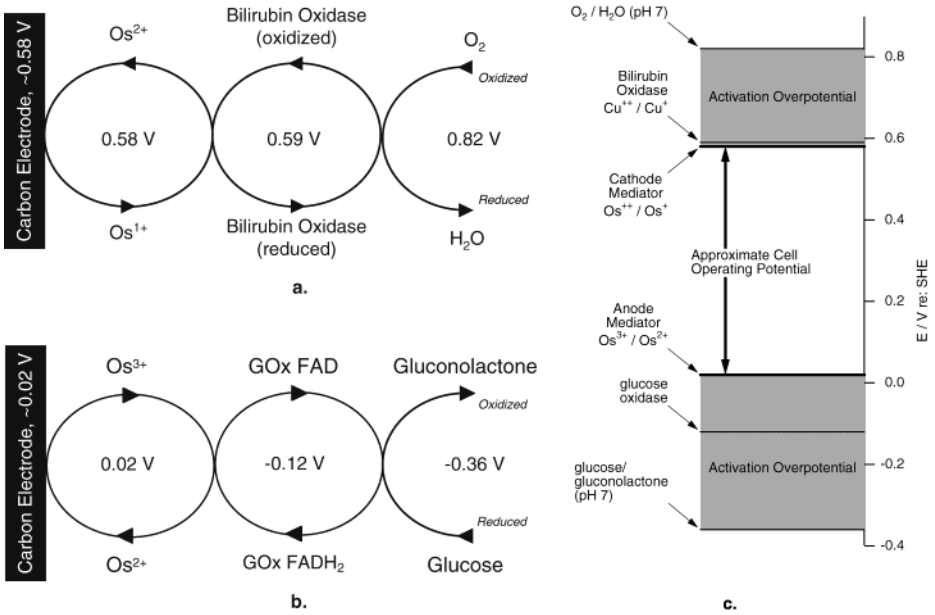

Figure 4. Potential schematic for a mediated biofuel cell. All potentials specified vs SHE.[110,126,182]

reaction conditions, rates of mediated electron transfer can exceed by orders of magnitude that of the direct mechanism. However, by introducing an additional transfer step, enzyme−mediator electron transfer is isolated from direct electrode potential control. For typically fast (Nernstian) kinetics between the mediator and electrode surface, the electrode potential merely controls the relative concentrations of oxidized and reduced mediator at the surface. At electrode potentials above its redox potential, mediator species in contact with the surface are primarily oxidized; below the redox potential, such species are primarily reduced. The electrode thus provides a boundary condition for electron flux to and from solution, which can occur either by mediator self-exchange or by bulk mediator diffusion. Both of these mechanisms are diffusional in nature and are therefore the result of gradients in concentration of oxidized and reduced mediator species.

The practical impact of such considerations is that the reversible potential of a mediated biocatalytic electrode is a mixed potential dominated by the mediator couple. By extension, the open-circuit potential of a biofuel cell comprising two such electrodes is primarily determined by the difference in redox potential of the two mediator couples. The difference in redox potential between the mediator and the consumed reactant represents a driving force for electron transfer and therefore must be nonzero. As shown in Figure 4 for a glucose−oxygen biofuel cell,[106] this difference represents an activation overpotential that reduces the observed open-circuit potential from a theoretical maximum, given by the formal potential difference between the fuel and oxidant. This reduction is in addition to that associated with driving electron transfer between each reactant and its respective biocatalyst.

Therefore, the range of appropriate mediators is limited to those with redox potentials close to that of the chosen enzyme. As previously discussed, mediator selection might also be dictated by other factors such as stability, toxicity, and biocompatibility. Using the format of free diffusion of the redox mediator (benzyl viologen) in solution, a methanol−dioxygen biofuel cell using NAD^+-dependent dehydrogenases can be found in the literature.[82] In a similar format, a laccase cathode using the redox mediator ABTS has been designed.[107] Although the format of free diffusion of the redox mediator is the most efficient method of MET, it necessitates semipermeable membranes or similar technology to retain the mediator near the electrode, limiting its practical application compared to other formats of MET. Despite the vast literature on other formats of MET,[73−78] the most successful format found in the literature, so far, is the design of miniature enzymatic biofuel cells based on "wired" biocatalysts, using osmium redox polymers.[26,106,108−110]

4.3.1. Diffusional Mediators

NAD(P)$^+$ as Anode Mediator. A majority of redox enzymes require the cation nicotinamide adenine dinucleotide, possibly phosphorylated (NAD(P)$^+$) as a cofactor. Of the oxidoreductases listed in *Enzyme Nomenclature*, over 60% have NAD(P)$^+$ as a reactant or product.[111,112] For example, methanol can be oxidized to form formaldehyde by methanol dehydrogenase (MDH, EC 1.1.1.244) according to

$$CH_3OH + NAD^+ \xrightarrow{MDH} CH_2O + NADH + H^+ \quad (1)$$

The reduced form, NADH, then releases electrons at an electrode surface, regenerating NAD$^+$, by

$$NADH \xrightarrow{electrode} NAD^+ + H^+ + 2e^- \quad (2)$$

NAD(P)$^+$ can function as a mediator for enzymatic anodes, except that the electrode potential required to reoxidize this molecule electrochemically is typically ~1 V positive of its formal oxidation potential (−320 ± 5 mV), leading to significant activation losses.[113,114] [Note that all potentials are reported relative to the standard hydrogen electrode (SHE). Potentials relative to Ag|AgCl in original references are adjusted by +0.22 V here.] Moreover, direct oxidation of NAD(P)H at an electrode surface results in fouling and deactivation of the electrode.[113,115] Thus, in systems utilizing NAD(P)$^+$, modified electrodes incorporating either a second biocatalytic cycle or a surface-bound oxidation catalyst are required for efficient oxidation of NAD(P)H. Sensor applications of NAD(P)$^+$-dependent enzymes have driven development of a broad range of mechanisms for NAD(P)H regeneration, and several excellent reviews are available in the literature.[80,116,117]

Palmore et al. applied the biocatalytic approach, utilizing the enzyme diaphorase (EC 1.6.4.3) to catalyze the reoxidation of NADH homogeneously, transferring electrons to a mediator, benzyl viologen.[82] The mediator was then reoxidized at an electrode surface, with the overall scheme

$$NADH + 2BV^{2+} \xrightarrow{DIA} NAD^+ + H^+ + 2BV^+$$

$$2BV^+ \xrightarrow{electrode} BV^{2+} + 2e^- \quad (3)$$

This approach was coupled to a system of three NAD$^+$-dependent enzymes comprised of alcohol dehydrogenase (EC 1.1.1.1), aldehyde dehydrogenase (EC 1.2.1.3), and formate dehydrogenase (EC 1.2.1.2) to create an electrode theoretically capable of complete oxidation of methanol to carbon dioxide, as shown in Figure 5. The anode was, in turn, coupled to a platinum-catalyzed oxygen cathode to produce a complete fuel cell operating at pH 7.5. With no externally applied convection, the cell produced power densities of 0.67 mW/cm^2 at 0.49 V for periods of less than 1 min, before the onset of concentration polarization.

A carbon felt electrode modified by electropolymerized methylene green has been implemented as the anode in an alcohol−O_2 biofuel cell.[48] The porous

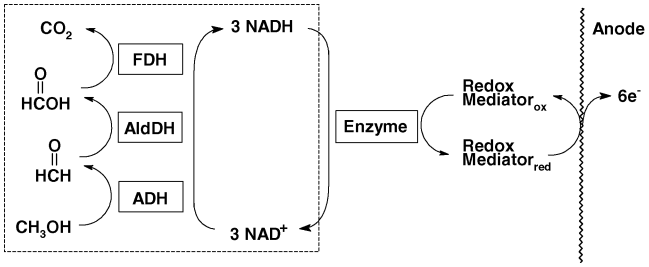

Figure 5. Oxidation of methanol to carbon dioxide by a three-enzyme system consisting of alcohol (ADH), aldehyde (AldDH), and formate (FDH) dehydrogenases. Each enzyme is NAD$^+$-dependent, and the NAD$^+$ is regenerated by the anode via a redox mediator system. Redrawn with permission from ref 82. Copyright 1998 Elsevier Science S.A.

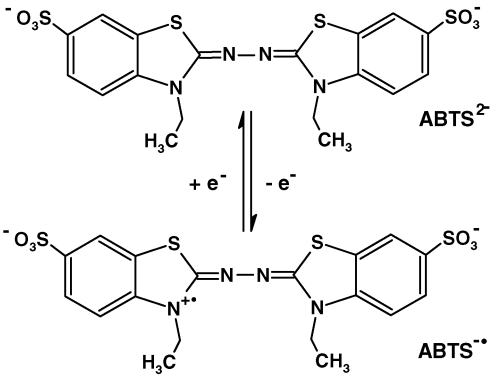

Figure 6. Structure of ABTS in reduced (ABTS^{2-}) and oxidized (ABTS$^{-\bullet}$) forms. Redrawn with permission from ref 107. Copyright 1999 Elsevier Science S.A.

electrode was coated with a Nafion suspension treated with tetrabutylammonium bromide to increase the local pH and the nanoscale pore size of the film, wherein a mixture of alcohol dehydrogenase and aldehyde dehydrogenase was immobilized. Power densities of up to 2 mW/cm^2 were obtained using an O_2/Pt cathode and ethanol as the fuel; using methanol, a power density of 1.5 mW/cm^2 was obtained. These bioanodes functioned for more than 30 days with less than 80% loss of activity.

ABTS as Cathode Mediator. Some recent efforts to construct biocatalytic oxygen electrodes have introduced 2,2′-azinobis(3-ethylbenzothiazoline-6-sulfonate), or ABTS, as a diffusional mediator for oxygen-reducing enzymes.[101] Having the structure shown in Figure 6 and Table 2 (compound **1**), ABTS^{2-} is introduced as a divalent anion that acts as a cosubstrate with oxygen-reducing enzymes having high redox potentials, such as laccase and bilirubin oxidase, oxidizing to a monovalent radical, ABTS$^{-\bullet}$, at a redox potential of 0.62 V vs SHE.

Palmore et al. first demonstrated the use of ABTS in a biofuel cell cathode, combining it with laccase from *Pyricularia oryzae*.[107] ABTS was dissolved at 2 mM in oxygen-saturated 0.2 M acetate buffer, pH 4, 25 °C. With a glassy carbon working electrode, an open-circuit potential of 0.53 V vs SCE was observed, reflecting the presence of HABTS$^-$ in low-pH solution. Protonation of ABTS^{2-} shifts the redox potential to 0.57 V vs SCE.[118] With negligible stirring, current densities of 100 μA/cm^2 were achieved at an electrode potential of 0.4 V vs SCE.

Table 2. Cathode Mediators

	Compound	Structure	Redox Potential (V)[a]	O_2 Reduction Rate (A/cm^2)[a,b]	Ref.
1	2,2′-azinobis (3-ethylbenzothiazoline-6-sulfonate) (ABTS)	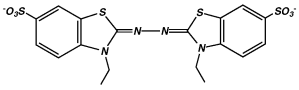	0.66, pH 4; 0.72, pH 7	5×10^{-4} (0.43 V, pH 7 phosphate)[c,e]	101,107,118
2	poly{*N*-vinylimidazole [Os(terpyridine) (4,4′-dimethyl-2,2′-bipyridine)]$^{2+/3+}$}	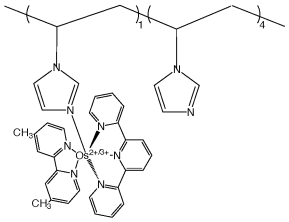	0.79, pH 5	1×10^{-2} (0.62 V, pH 5 citrate)[d,f]	10,26
3	poly{*N*-vinylimidazole [Os(4,4′-dichloro-2,2′-bipyridine)$_2$Cl]$^{+/2+}$ -*co*-acrylamide}	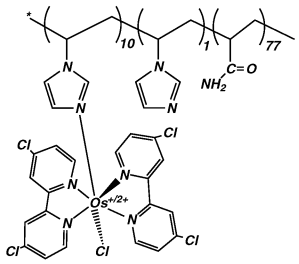	0.58, pH 7.4	9×10^{-3} (0.55 V, pH 7 phosphate)[c,f]	109,110,166

[a] Potentials vs SHE. [b] High-surface-area carbon supports in O_2-saturated buffer. [c] Catalyzed by bilirubin oxidase in the presence of chloride. [d] Catalyzed by fungal laccase, chloride absent. [e] Moderate stirring by bubbled gas. [f] Strong stirring by rotating disk electrode at 4 krpm.

At 0.44 V vs SCE, the redox potential of ABTS falls well below that of the Cu^{2+}/Cu^{+} couple of laccase (0.54 V vs SCE, pH 4). It is, however, well matched to that of bilirubin oxidase (BOD) another copper-centered, oxygen-reducing enzyme. In contrast to laccase, BOD provides an added benefit of near-peak activity at neutral pH.[101,109] Tsujimura et al. employed ABTS for mediation of O_2 reduction catalyzed by bilirubin oxidase from *M. verrucaria*.[101] Voltammetry was conducted using a glassy carbon electrode in air-saturated pH 7 phosphate buffer, 25 °C, containing 0.25 mM $ABTS^{2-}$ and 0.11 μM BOD. Current densities approaching 40 $\mu A/cm^2$ were observed. Observation of maximum current density for $ABTS^{2-}$ concentrations up to 1.5 mM yielded current densities exceeding 100 $\mu A/cm^2$ and effective Michaelis−Menten parameters of $k_{cat} = 820/s$ and $K_{ABTS} = 11$ μM. A similar study of oxygen concentration yielded $K_{O_2} = 51$ μM, much less than the air-saturated concentration of oxygen in the buffer (~250 μM). When a high-surface-area carbon felt sheet was used as a working electrode in O_2-saturated buffer containing 0.5 mM $ABTS^{2-}$ and 0.11 μM BOD, current densities of up to 900 $\mu A/cm^2$ were observed, and a similar current density was obtained in air because of the low value of K_{O_2}.

Although the diffusion coefficient ($D_{ABTS} = 3.2 \times 10^{-6}$ cm^2/s) and solubility (>30 mM) of $ABTS^{2-}$ are much higher than those of competing redox polymers, the compound was found to suffer from oxidative degradation at potentials exceeding 0.92 V vs SHE in pH 7 buffer.[101] Cyclic voltammetry of $ABTS^{2-}$ detected two oxidation peaks, one at 530 mV that was reversible and one near 1 V that was reversible at high scan rate (20 V/s) and irreversible at low scan rate (1 V/s). The reversible peak at 530 mV was associated with the one-electron oxidation of $ABTS^{2-}$ to $ABTS^{\bullet-}$, and the higher-potential, irreversible peak was associated with oxidation of $ABTS^{\bullet-}$ to neutral ABTS. Bulk electrolysis for 20 min at 1.0 V led to the elimination of all peaks, suggesting that ABTS is decomposed at high potential by an unknown mechanism.

Homogeneous, BOD-catalyzed oxygen reduction in the presence of $ABTS^{2-}$, presumably according to the reaction

$$4ABTS^{2-} + O_2 + 4H^+ \Rightarrow 4ABTS^{\bullet-} + 2H_2O \quad (4)$$

was monitored using a Clark-type oxygen electrode. The reaction proceeded rapidly up to the limit of depletion of $ABTS^{2-}$ according to eq 4, but thereafter, it continued to consume oxygen, albeit at a lower rate. The authors suggested that $ABTS^{2-}$ might be slowly regenerated by disproportionation of the radical $ABTS^{\bullet-}$

$$2ABTS^{\bullet-} \Rightarrow ABTS^{2-} + ABTS \quad (5)$$

where the neutral ABTS decomposes as mentioned above. Thus, the redox-active ion is regenerated, but the total ABTS concentration is irreversibly depleted, the process occurring over a time scale of minutes to hours.

4.3.2. Immobilized Mediators

It is desirable to contain enzymes and electron-transfer mediators within an electrode volume to

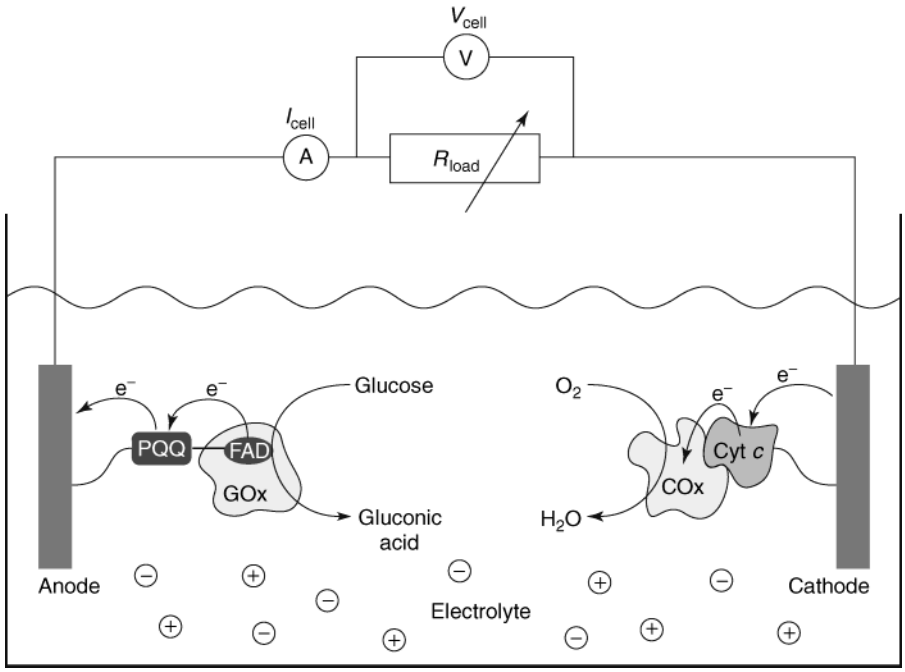

Figure 7. Noncompartmentalized glucose−oxygen biofuel cell. Reprinted with permission from refs 12 and 125. Copyright 2003 John Wiley and Sons Limited. Copyright 1999 Elsevier Science S.A.

maintain concentration and activity. In the case of diffusional mediators, this requires the use of semipermeable barriers such as polymer membranes, intended to prevent flux of mediator species out of the electrode. However, these membranes also limit the diffusional flux of reactants into and products out of the electrode. Such diffusional limitations might be desirable in the context of an enzymatic sensor, where limiting current can be monitored for amperometric detection of a reactant. In a biofuel cell, however, such limitations lead to performances losses, and diffusional barriers are, in principle, to be avoided.

An alternative containment scheme is immobilization of active species on a surface[119−125] or within a tethered polymer brush or network.[10,13,126,127] Surface immobilization can achieve high surface utilization by locating mediators and biocatalysts within nanometers of conducting surfaces. Immobilization on polymer networks allows for dense packing of enzymes within electrode volumes at the expense of long-distance electron mediation between the enzyme active center and a conductive surface. Such mediation often represents the rate-limiting step in the overall electrode reaction.

Examples of surface-immobilized mediators are electropolymerized azines for electro-oxidation of NADH.[119,120] The extreme form of this approach is formation of biocatalytic monolayer, comprising a surface-bound mediator species that is itself bound to a single enzyme molecule. Katz et al. report a complete cell based on novel architecture at both electrodes (Figure 7).[125] On the anode side, the FAD center of glucose oxidase is removed from the enzyme shell and covalently attached to a pyrroloquinoline quinone (PQQ) mediator species previously immobilized on a gold surface. The GOx apoenzyme (enzyme with active center removed) is reintroduced in solution and selectively binds to FAD, resulting in a PQQ-mediated GOx monolayer with physical attachment of its FAD center to the electrode surface.[128] On the cathode side, a similar approach is taken wherein cytochrome *c* is immobilized on a gold surface by site-specific covalent bonding to a maleimide monolayer.[129] This monolayer was then exposed to cytochrome oxidase, which complexed with the cytochrome *c* and was subsequently cross-linked with glutaric dialdehyde. A cell combining these two electrodes, operating in 1 mM glucose and air-saturated buffer at pH 7 and 25 °C, generated a maximum current density of 110 μA/cm^2 at 0.04 V cell potential.

More frequently in the literature, labile redox complexes based on osmium or ruthenium are immobilized on water-soluble polymers such as poly(vinyl imidazole) or poly(allylamine), which can, in turn, be immobilized on a surface such as a Langmuir−Blodgett film,[130,131] chemically cross-linked,[126,132−135] or electropolymerized[127] to form a hydrogel. In such structures, the mobility of the polymer backbone provides restricted translational mobility to the redox complex, allowing electron transport via exchange between neighboring centers while preventing their bulk diffusion.[136,137] Such a scheme leads to electron transport that, in the absence of significant potential gradients (achieved at low current density or by the presence of a supporting electrolyte), can be characterized as a diffusional process and quantified by an apparent diffusion coefficient.[138] Historically, a major drawback of redox polymer electron mediators has been measured values of apparent diffusion that fall in the 10^{-9}−10^{-8} range, orders of magnitude lower than those of diffusional species.[139,140] Recently, an additional degree of translational freedom has been demonstrated in redox polymers wherein the complex is attached to the polymer backbone via a long tether.[126]

Choice of an effective mediator to shuttle electrons between the enzyme active site and the electrode involves several criteria: The mediator must be stable in both oxidized and reduced forms, must engage in rapid electron transfer with the biocatalyst and at the interface with a conducting material, and must have a redox potential allowing the electrode to be poised appropriately to avoid unwanted reactions and minimize overpotential.[141] Bipyridine- and terpyridine-based chelates of osmium(II/III) fulfill all of these requirements. In addition, electron-donor characteristics of the ligands effectively tune the redox potential of the metal center,[142,143] allowing one to engineer the mediator at the molecular level to work in conjunction with a desired enzyme. In general, synthesis can be accomplished by adding the stoichiometric amounts of ligand and osmium chloride salt $(NH_4)_2OsCl_6$ and refluxing in ethylene glycol.[144]

Osmium generally has a coordination number of six. Complexes of osmium with a chloride remaining in their coordination sphere after addition of the ligands can further be complexed with a pendant group in a polymer, thus producing a *redox polymer*.[145] By choosing a water-soluble polymer backbone that can be cross-linked, one can produce a *redox hydrogel* in an aqueous environment. In this state, the osmium complexes retain their ability to mediate for the enzyme.[146] The polymer binds to the electrode surface by a van der Waals interaction, and the enzyme is immobilized in the redox hydrogel by electrostatic forces or by covalent cross-linking, thus making the system resistant to flow-induced shear.

Redox polymers, defined as polymer molecules that include locally redox-active sites, have been known since at least the 1960s[147] and were incorporated into modified electrodes in the early 1980s.[148] Redox polymers were first employed for immobilization and mediation of redox biocatalysts by the Heller group, in the context of amperometric biosensors.[149] After the external shell of glucose oxidase had first been covalently modified with a variety of redox relays, it was found that approximately 10−20 relay sites could be attached to each protein molecule. This was found to be insufficient for a substantial increase in electron-transfer efficiency, primarily because such a low density of transfer sites did not eliminate the orientation dependence for electron transfer.[150−152] In contrast, electrostatic complexation of the polyanionic glucose oxidase with a polycationic redox polymer—such as poly(vinylpyridine) partially complexed with $[Os(2,2'\text{-bipyridine})_2Cl]^{+/2+}$ and partially *N*-methylated—led to modified electrodes with a *bulk* enzyme/relay ratio in excess of 10^3.[153] Such electrodes produced glucose oxidation current densities of up to 30 $\mu A/cm^2$ that were proportional to glucose concentration up to 30 mM.

More recently, osmium-based redox polymers of similar structure have been developed as mediators for enzyme-catalyzed reactions relevant to biofuel cells. In this context, the chief development objectives have been tuning the redox potential for both anodes and cathodes and improving electron-transfer efficiency.

Trudeau et al. reported the earliest redox-polymer-mediated laccase electrode, in the context of an inhibition biosensor.[154] The electrode consisted of laccase from *T. versicolor* coimmobilized with poly(*N*-vinylimidazole), or PVI, complexed with $Os(bipyridine)_2Cl_2$.[155] Current densities of 3.5 $\mu A/cm^2$ were observed at an electrode poised at 0.42 V vs SHE in oxygen-saturated, room-temperature acetate buffer, pH 4.7. Building on this work, a polymer composed of PVI complexed with Os(dimethylbipyridine)(terpyridine) was synthesized (Table 2, compound **2**).[10,108] Introducing the terpyridine ligand to eliminate chloride ligands increased the redox potential of 0.77 V vs SHE at pH 5, close to the observed redox potential of fungal laccase. Electrodes composed of laccase and this redox polymer generated current densities of 1.2 mA/cm^2 on a glassy carbon rotating disk electrode (RDE) in well-stirred, oxygen-saturated citrate buffer, pH 5. The polymer−laccase adduct was then coated on a carbon paper support of 350-μm thickness, mounted on a rotating disk electrode (RDE). When rotated at 4000 rpm to provide substantial stirring, current densities of 7 mA/cm^2 were obtained. Current decay rates of 40% and 17% per day were observed, respectively, for the glassy carbon and carbon paper electrodes on rotating disk electrodes rotating at 1000 rpm.

A similar polymer, composed of osmium complexed with bis-dichlorobipyridine, chloride, and PVI in a PVI−poly(acrylamide) copolymer (Table 2, compound **3**), demonstrated a lower redox potential, 0.57 V vs SHE, at 37.5 °C in a nitrogen-saturated buffer, pH 5.[109,156] An adduct of this polymer with bilirubin oxidase, an oxygen-reducing enzyme, was immobilized on a carbon paper RDE and generated a current density exceeding 9 mA/cm^2 at 4000 rpm in an O_2-saturated PBS buffer, pH 7, 37.5 °C. Current decayed at a rate of 10% per day for 6 days on an RDE at 300 rpm. The performance characteristics of electrodes made with this polymer are compared to other reported results in Table 2.

This electrode is unique in that the bilirubin oxidase is active at neutral pH, whereas the laccase cited above is not, even though the redox potential of laccase is somewhat higher. Additionally, the bilirubin oxidase is much less sensitive to high concentrations of other anions such as chloride and bromide, which deactivate laccase.[25,26] It was shown that mutations of the coordination sphere of bilirubin oxidase led to an increased redox potential of the enzyme, which increased current density and reduced current decay to 5%/day over 6 days at 300 rpm.[157] The latter improvement was attributed to improved electrostatic attraction between the enzyme and the redox polymer. An electrode made with high-purity bilirubin oxidase and this redox polymer has recently been shown to outperform a planar platinum electrode in terms of activation potential and current density of oxygen reduction.[179]

A recently reported immobilization approach involved the entrapment of the cyano-metal complexes $[Fe(CN)_6]^{3-/4-}$, $[W(CN)_8]^{3-/4-}$, $[Os(CN)_6]^{3-/4-}$, and

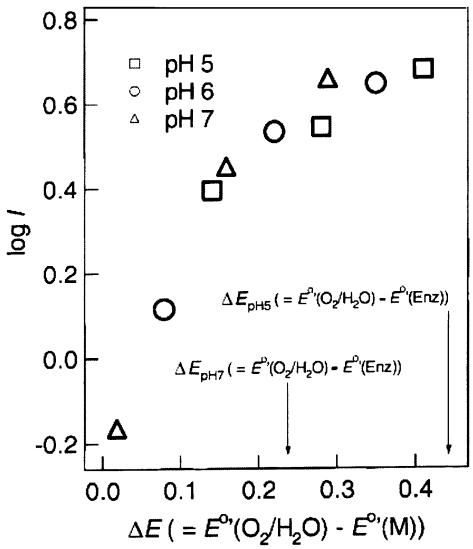

Figure 8. Dependence of the BOD-catalyzed oxygen reduction current density on the difference in formal potentials between the O_2/H_2O couple and a range of cyano-metal complexes (M) for three values of solution pH. Arrows indicate reported values of the BOD formal potential $E^{0'}$(Enz) relative to that of O_2/H_2O. Reproduced with permission from ref 159. Copyright 2003 Elsevier Science B.V.

$[Mo(CN)_8]^{3-/4-}$ within a poly(L-lysine) matrix.[158,159] Similarly to the redox polymer backbones PVI and quaternized poly(vinylpyridine), the poly(L-lysine) is cationic, and immobilization of anionic cyano-metal complex within the polymer matrix was accomplished via electrostatic attraction. Formal redox potentials obtained in room-temperature phosphate buffer at pH 7 were from 0.24, 0.52, 0.69, and 0.78 V for the Fe, W, Os, and Mo cyano complexes, respectively. Cyclic voltammetry of a glassy carbon electrode in an oxygen-saturated solution of the W, Os, and Mo cyano complexes and bilirubin oxidase (BOD) showed a direct correlation between the observed biocatalytic oxygen reduction current and the formal potential difference between the mediator and the O_2/H_2O couple. As shown in Figure 8, this relationship was independent of solution pH. The formal potential of the $Cu^{+/2+}$ center of BOD was less than that of the Os- and Mo-centered mediators at pH 7. Catalytic oxygen reduction currents were nonetheless observed and were attributed to the overall potential drop. Such an interpretation is consistent with the discussion of Figure 3 above, as the potential difference between the mediator and the reacting species represents the driving force, or activation overpotential, for the electrochemical half-reaction.

When $[W(CN)_8]^{4-/3-}$ was coimmobilized with BOD and poly(L-lysine) on carbon felt sheet of 1-mm thickness on an RDE, a current density of 17 mA/cm^2 was observed at 0.4 V and 4000 rpm in oxygen-saturated phosphate buffer, pH 7. The authors partially attribute the high current density to convective penetration of the oxygen-saturated solution within the porous carbon paper electrode. This assertion is justified by calculation of an effective electrode area based on the Levich equation that exceeds the projected area of the experimental electrode by 70%.[160] This conclusion likely applies to any highly porous electrode that extends from the surface of an RDE into solution to a distance greater than the mass-transfer boundary layer thickness, which, for transport of O_2 from saturated solution at 1000 rpm, is about 20 μm.[161]

Osmium-based redox polymers designed for glucose anode applications have been developed using a similar approach. Based on polymers designed to mediate glucose oxidase, horseradish peroxidase, and other redox enzymes for sensor applications,[132,162] attention was focused on reducing the redox potential of the mediator to match that of glucose oxidase (approximately −0.4 V vs SHE for the dissolved enzyme, −0.3 V vs SHE for enzyme adsorbed on carbon)[163] and improving transport properties while maintaining high activity with respect to the enzyme. Table 3 gives properties and performances of four redox polymers implemented in glucose-oxidizing biofuel cell anodes.

Compounds **4** and **5** of Table 3, implementing methylated[106,164] and methoxylated[165,166] bipyridine ligands to the osmium center, were borrowed directly from previous, sensor-targeted chemistries. The redox potentials of these polymers are high, exceeding 0.1 V vs SHE. A high redox potential provides a strong driving force for reoxidation of the GOx enzyme, indicated by current densities exceeding 200 μA/cm^2, yet reduces the overall cell potential.

These redox polymers were modified for reduced redox potential while maintaining activity with GOx. Replacement of the methyl groups (compound **4**) with amines (compound **6**) resulted in a redox potential decrease of 0.25 V, with only a 15% loss in GOx activity. More recently, further reductions in redox potential were achieved by replacing the bipyridine ligands to osmium by dimethylated bis-imidazole groups (compound **7**).[126]

Further, the electron-transport properties of the polymer **7** were enhanced by extending the separation between the redox center and backbone from a single Os−amino linkage to one that extends over 17 bonds. The goal was to provide mobility of the redox center independently of backbone motion, which is necessarily restricted by cross-linking. The mobility of the redox center can be characterized by an apparent diffusion coefficient, D_{app}. According to the relation proposed by Blauch and Saveant[136,137]

$$D_{app} = \frac{1}{6}k_{ex}(\delta^2 + 3\lambda^2)C_T \qquad (6)$$

where k_{ex} is a rate constant for electron self-exchange between redox centers, δ is the center−center distance during exchange, λ is the average center displacement from its equilibrium position, and C_T is the total redox center concentration. When a redox center is tethered to a polymer backbone by a short linkage, λ depends primarily on the range of mobility of the backbone itself.

From a basic standpoint, an increased linkage length, N, can increase the value of λ by partially decoupling the motion of the redox center from that of the backbone. In an ideal case, with a well-solvated linkage that does not impair backbone mobility, the value of λ^2 should vary with N. In reality, such

Table 3. Redox Polymer Anode Mediators

	Compound	Structure	Redox Potential (V)[a]	Glucose Oxidation Rate, (A/cm^2)[a,b]	Ref.
4	Poly{*N*-vinylimidazole [Os(4,4´-dimethyl-2,2´-bipyridine)$_2$Cl]$^{+/2+}$ -*co*-acrylamide}	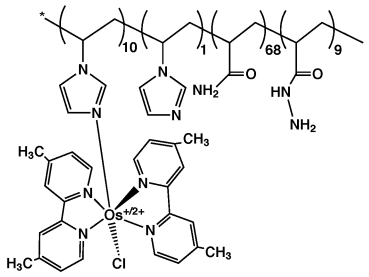	0.32, pH 5 0.17, pH 7.2	2×10^{-4} (0.5 V, pH 5 citrate)	106,164
5	poly{*N*-vinylpyridine [Os(4,4´-dimethoxy-2,2´-bipyridine)$_2$Cl]$^{+/2+}$}	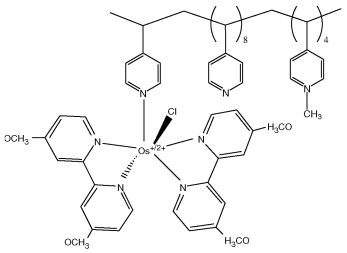	0.15, pH 7.4	6.5×10^{-4} (0.37 V, pH 7.4 PBS[c])	165,166
6	poly{*N*-vinylimidazole [Os(4,4´-diamino-2,2´-bipyridine)$_2$Cl]$^{+/2+}$}	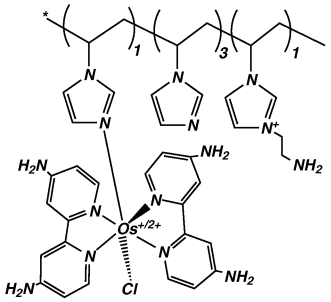	0.06, pH 7.4	1.7×10^{-4} (0.22 V, pH 7.4 PBS)	110
7	Poly{*N*-vinylpyridine [Os(*N*,*N*´-dialkylated-2,2´-biimidazole)$_3$]$^{2+/3+}$}	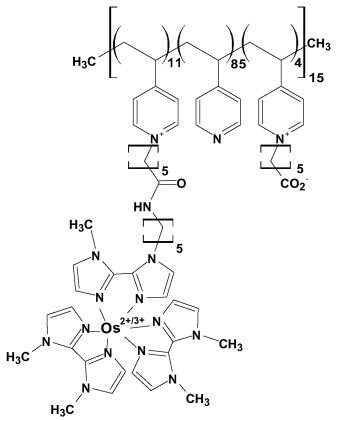	0.02 pH 7.2	1.1×10^{-3} (0.22 V, pH 7.2 PBS); 3.2×10^{-4} (0.22 V, pH 5 citrate)	126,156,168

[a] Potentials vs SHE. [b] Glucose concentration 15 mM, 37 °C. [c] PBS = phosphate buffer solution, typically 20 mM phosphate buffer with 0.1 M NaCl.

changes to polymer structure can have a dramatic impact on backbone dynamics because of increased drag and steric effects and can also impact cross-linking efficiency and solvent interactions. However, such an approach provides an opportunity to increase the low observed values of D_{app} in redox polymers, typically in the 10^{-8}–10^{-9} cm^2/s range.

The long linkage in compound **7** led to an apparent diffusion coefficient, D_{app}, that was a factor of 10^3 higher than the $\sim10^{-9}$ cm^2/s observed for compound **6**, as shown in Figure 9. However, the D_{app} value of the long-linkage polymer was more sensitive to the degree of cross-linking of the backbone, decreasing by 95% as the cross-linker mass fraction was increased from 0 to 25%. Over the same range, the short-linkage redox polymer experienced a 50% decrease in D_{app}. Despite the increased sensitivity to cross-linking, compound **7** still displayed a D_{app} value that was 2 orders of magnitude higher than that of compound **6** under highly cross-linked conditions. As

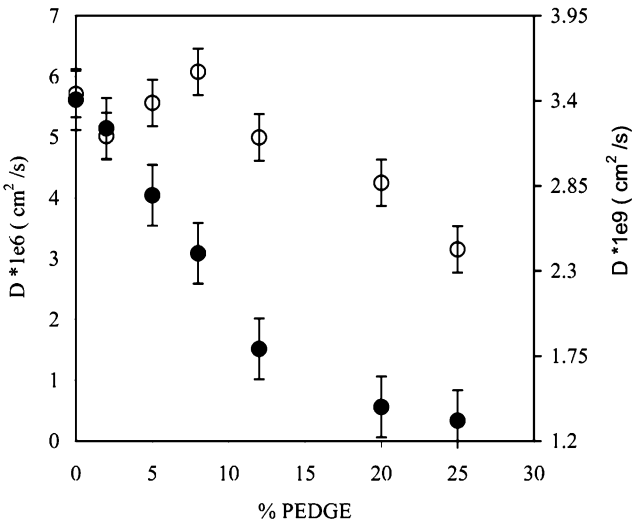

Figure 9. Dependence of D_{app} of compound **6** (○, right axis) and compound **7** (●, left axis) on the weight fraction of the cross-linker. Obtained by cyclic voltammetry and potential-step chronoamperometry on a 3-mm-diameter glassy carbon electrode under argon: 0.1 M NaCl, 20 mM phosphate buffer, pH 7, 37 °C, 20 mV/s. Reprinted with permission from ref 126. Copyright 2003 American Chemical Society.

shown in Table 3, the resulting activity with respect to GOx increased by a factor of 5 to ~1 mA/cm^2.

5. Engineering of Enzymatic Biofuel Cell Systems

The recent literature in bioelectrochemical technology, covering primarily the electrochemical aspects of enzyme immobilization and mediation, includes few reports describing engineering aspects of enzymatic biofuel cells or related devices. Current engineering efforts address issues of catalytic rate and stability by seeking improved kinetic and thermodynamic properties in modified enzymes or synthesized enzyme mimics. Equally important is the development of materials and electrode structures that fully maximize the reaction rates of known biocatalysts within a stable environment. Ultimately, the performance of biocatalysts can be assessed only by their implementation in practical devices.

5.1. Complete Enzymatic Fuel Cells

Several references discussed above[48,82,107] describe voltaic cells coupling a biocathode or bioanode with a noble metal counter electrode that can be reasonably considered biofuel cells. However, additional levels of difficulty arise when preparing cells containing two bioelectrodes simultaneously[84,101,121,123,167] and when coupling the two electrodes, composed of differing enzyme systems, in common conditions of pH, temperature, and electrolyte.[106,110,125,166,168] Three key recent reports where this was achieved are discussed below.

Already mentioned was a complete cell reported by Katz et al. based on monolayer immobilization of mediator and biocatalyst at both anode and cathode (Figure 7).[125] Operating in 1 mM glucose and air-saturated buffer at pH 7 and 25 °C, the cell generated a maximum current density of 110 μA/cm^2 at 0.04 V cell potential, corresponding to a maximum power of 5 μW/cm^2. The observed low power is expected because of the monolayer quantity of immobilized enzymes at each electrode, the planarity of the gold substrates, and low redox potential of cytochrome oxidase. However, the significant achievement of active-site-directed binding of biocatalyst at both electrodes in common solvent is notable.

More recently, Tsujimura et al. reported a H_2/O_2 fuel cell operating at pH 7, based on methyl viologen-mediated bacterial cells (*Desulfovibrio vulgaris*) at the anode and ABTS-mediated bilirubin oxidase at the cathode.[83] Although beyond the scope of this review in a strict sense, this report is notable as it is the first report of a biocatalyst-based fuel cell operating at pH 7. At both electrodes, carbon felt sheets were immersed in solutions containing pH 7 phosphate buffer and freely diffusing catalysts and mediators, and an anion-exchange membrane separated the two compartments. An open-circuit potential of 1.17 V was reported, which is generally higher than similar observations made of noble-metal-based proton exchange membrane fuel cells operating at much higher temperatures. A limiting current due to transport at the cathode was observed at 0.45 mA/cm^2, a value that was doubled by doubling the concentration of cathode biocatalyst and mediator. In addition to low current density, the short lifetime (~2 h) of this device was noted as an issue.

The authors have also recently reported a compartmentless glucose−oxygen cell relying on pyrroloquinoline quinone (PQQ) mediated soluble glucose dehydrogenase (sGDH) for anodic oxidation of glucose.[169] Although unstable compared to glucose oxidase, sGDH is insensitive to the presence of oxygen and delivers higher activity. A maximum power density of 0.058 mW/cm^2 was achieved at neutral pH.

Heller and co-workers have published a series of papers based on a miniature membraneless biofuel cell operating on glucose and oxygen.[106,110,156,166,168] All of the devices consisted of enzymatic electrodes immobilized within and mediated by osmium-based redox hydrogels deposited on 7-μm-diameter carbon fibers. The fixture for these devices is shown in close-up in Figure 10. The original device consisted of glucose oxidase mediated by a poly(vinylimidazole)−poly(acrylamide) copolymer (PVI−PAM) complexed with Os(dimethylbipyridine)$_2$Cl at the anode and fungal laccase mediated by PVI complexed with Os(dimethylbipyridine)(terpyridine). These electrodes have been discussed individually in previous sections. The complete cell operated in pH 5 citrate buffer saturated with air and containing 15 mM glucose. At a cell potential of 0.4 V, current densities of 160 and 340 μA/cm^2 were obtained at 23 and 37 °C, respectively, limited primarily by anode performance. Current density decreased by ~8% per day over 3 days.

The fuel cell described above exhibited three key flaws. First, the anode redox mediator operates at a redox potential well above that of glucose oxidase, raising the operating potential of the anode and lowering the achievable cell potential. Second, the cell operates at pH 5, near-optimal for the laccase electrode but suboptimal for the current-limiting glucose

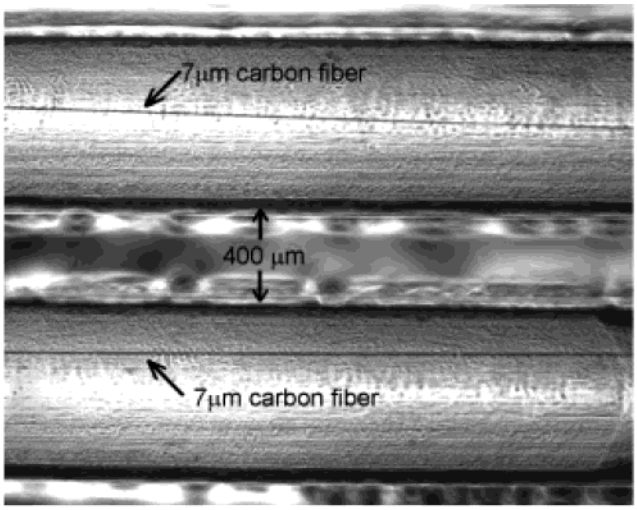

Figure 10. Miniature biofuel cell segment consisting of mediated enzymes immobilized on 7-μm-diameter fibers. Reprinted with permission from ref 106. Copyright 2001 American Chemical Society.

anode. Third, at typical thicknesses of deposited hydrogel films, electron transport via the redox mediator is the rate-limiting step. Later authors have reported improvements on this design by incorporating alternative enzymes and novel redox mediators that overcome these limitations.

For example, the small scale of the device was intended as a demonstration of architecture suitable for implanted applications. Mano et al. demonstrated a miniature fuel cell with bilirubin oxidase at the cathode catalyst that is more active at pH 7 and tolerates higher halide concentrations than does laccase.[156] Additionally, the long-side-chain poly(vinylpyridine)−Os(dialkyl-bis-imidazole)$_3$ redox polymer discussed above was employed to both lower the anode potential and, via the long side chains, enhance electron transport from the biocatalyst. The cell achieved a current density of 830 μA/cm^2 at 0.52 V and 37 °C in an air-saturated, pH 7 buffer with 15 mM glucose. Thus, power density was more than doubled over the previous design. The stability of the cell was somewhat similar to that of the original cell at 6% current density loss per day over 6 days.

5.2. Electrode Structures

Electrodes for biological fuel cells generating 1 W or greater are expected to be composite structures comprising biocatalysts immobilized on or near the surface of porous conducting solid materials, probably carbon or possibly gold. Therefore, just as in conventional porous fuel cell electrodes, issues of transport to, from, and within these structures are expected to be significant. The challenges go beyond the domain of conventional fuel cells in that enzyme catalysts must generally be maintained within an aqueous phase. Issues of electron transfer within the aqueous phase automatically arise. Additionally, the size, activity, and packing density of biocatalytic active centers can require electrode thicknesses on the order of 100 μm (discussed below), leading to performance limitations associated with transport of reactants and products. The typical diffusion driving force, the

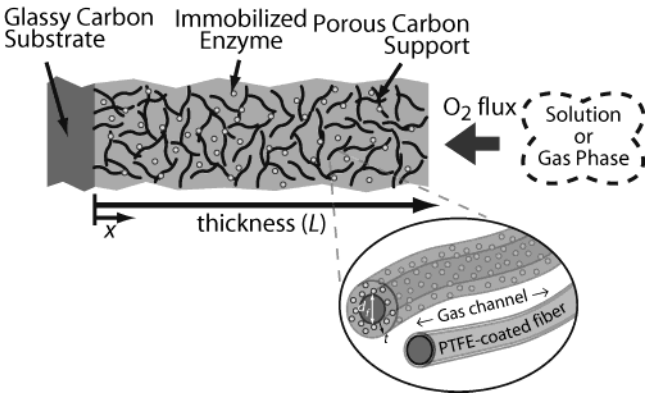

Figure 11. One-dimensional model diagram for supported laccase cathode.[170]

diffusion coefficient multiplied by the bulk concentration, is 10^{-11} mol·cm^{-1}·s^{-1} for both glucose and oxygen in water. These values lead to limiting current densities of order 100 μA/cm^2 through such systems, making the engineering of enzyme-immobilizing electrodes for reactant transport crucial to realizing high power density.

A model of such structures has been proposed that captures transport phenomena of both substrates and redox cosubstrate species within a composite biocatalytic electrode.[170] The model is based on macrohomogeneous and thin-film theories for porous electrodes and accounts for Michaelis−Menton enzyme kinetics and one-dimensional diffusion of multiple species through a porous structure defined as a mesh of tubular fibers.[85,171,172] In addition to the solid and aqueous phases, the model also allows for the presence of a gas phase (of uniformly contiguous morphology), as shown in Figure 11, allowing the treatment of high-rate gas-phase reactant transport into the electrode.

When applied to a laccase-based oxygen-reducing electrode, the model predicted a maximum current density of 9.2 mA/cm^2 at 0.6 V vs SHE for a 300-μm-thick electrode relying on transport of oxygen by diffusion in the liquid phase. However, when either convective transport in the liquid phase or gas-phase diffusive transport was introduced in the electrode, current densities exceeding 50 mA/cm^2 were predicted for air-saturated systems. As is evident in Figure 12, such electrodes will require thicknesses exceeding 100 μm and porosities exceeding 90%, with 25% porosity reserved for the gas phase in a gas diffusion electrode. This work points to enhanced reactant transport as an essential component to high-rate biocatalytic electrodes.

The design of biocatalytic electrodes for activity toward gaseous substrates, such as dioxygen or hydrogen, requires special consideration. An optimal electrode must balance transport in three different phases, namely, the gaseous phase (the source of substrate), the aqueous phase (where the product water is released and ionic transport takes place), and the solid phase (where electronic transport occurs). Whereas the selectivity of biocatalysts facilitates membraneless cells for implementation in biological systems that provide an ambient electrolyte,[13] gas-diffusion biofuel cells require an electro-

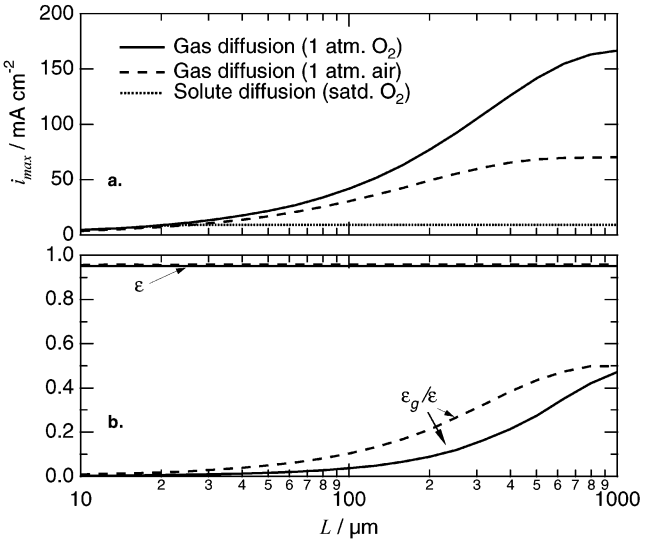

Figure 12. Effect of electrode thickness on performance of an oxygen-reducing laccase electrode: (a) optimum current density, i_{max}, at 0.5 V vs SHE and (b) optimum support porosity (ϵ) and relative gas-phase porosity (ϵ_g/ϵ) for carbon fiber supported electrodes optimized for (—) gas diffusion in 1 atm O_2, (– – –) gas diffusion in 1 atm air, (···) solute diffusion in O_2-saturated electrolyte. Dissolved oxygen diffusion favors thin electrodes. Gas diffusion favors thick electrodes, particularly in pure O_2.[170]

lytic phase to accomplish ion transfer between electrodes. The electrolyte can be present either as a liquid or more frequently as a liquid-permeable polymer membrane. A liquid phase is also needed to hydrate the biocatalyst, and hydration levels of hydrophilic polymers such as proteins and hydrogels that contact vapor-phase water are significantly lower than when in liquid contact, owing to the well-known Schroeder effect.[173] Finally, as described above, a hydrophobic phase must be maintained to facilitate gas transport through the electrode. Engineering all of these features into a stable, high-rate gas-phase biocatalytic electrode remains a tremendous challenge.

6. Future Outlook

As Heller and others have stated, the development of successful power sources has always been driven by demand arising from specific applications.[13] The technological paths to successful biofuel cells will therefore be determined by application specifics: Implanted biofuel cells must exhibit biocompatibility, and cathodes for ex vivo electronics must take advantage of gas-phase oxygen. That being said, a general truth remains: The advantages of biofuel cell technology will compel adoption in any application only if its disadvantages relative to conventional technology are minimal. It is clear that the advantages of biocatalysts are reactant selectivity, activity in physiological conditions, and manufacturability. The weaknesses are equally clear: modest absolute activity and low stability. These two issues are of significance, to a greater or lesser extent, in every conceivable application of this technology.

In our view, there exist two complimentary and overlapping paths toward addressing these issues: engineering of the protein molecule itself and engineering of the environment in which the molecule is expected to be active. These paths overlap primarily in that they require significant fundamental understanding of the enzyme molecule for progress to be made. Biomimetic techniques are under rapid development as a means to probe mechanistic aspects of biocatalysis.[174−177] However, the biomimetic approach has not yet produced practical biocatalysts, mainly because, so far, synthesized analogues are more expensive, less active, and more unstable than the natural enzyme. Through such approaches, we have progressed toward understanding transition state stabilization and transport processes at enzyme active sites. However, we generally lack an understanding of how the environment formed by inactive groups impacts the mechanism and stability of activation.

Similarly, efforts to increase enzyme stability by encapsulation in hydrophilic sol−gel matrixes yield the desired stability, generally at the expense of lower absolute activity.[5,6] The charged surface and small pores of the gel are thought to inhibit denaturation while partially reducing the dynamic motion of entrapped biomolecules and reducing transport and access of substrates to active sites. Engineering of enzyme molecules and immobilization environments will therefore benefit greatly from increased understanding of protein structure−function relationships. Clear understanding of the thermodynamics and dynamics of enzyme molecules such as glucose oxidase, bilirubin oxidase, laccase, and NAD-dependent redox enzymes will lead to new techniques for biomimetics, immobilization, and stabilization of activity. Fortunately, such research is also driven by myriad other potential applications.

As mentioned above, one of the primary challenges at hand is increased biocatalytic power density. Currently available enzymes provide sufficient intrinsic activity. An enzyme of 100-nm^2 cross section with an activity of 500 electrons per second generates a current density of 80 μA/cm^2 at monolayer loadings, comparable to the results of Katz et al.[125] For practical biofuel cells operating at current densities above 10 mA/cm^2, loadings of such an enzyme equivalent to hundreds or thousands of monolayers will be required. Assuming 100 kDa molecular weight, a 1 mg/cm^2 loading—the equivalent of 6000 monolayers or 60-μm thickness—has a theoretical maximum current density of 500 mA/cm^2. Thus, a key question is how to achieve significant biocatalyst utilization at such loadings, which leads to issues of transport of electrons and substrates within the electrode structure.

A key challenge is electron mediation. Currently, most mediated systems demonstrate high initial activity but introduce an additional source of long-term instability. There is a strong need for improved mediators that can be immobilized for retention, have high chemical and mechanical stability, and maintain high biocatalytic activity at low catalyst−mediator overpotentials. Redox hydrogels have shown great promise in the context of electron transport and redox potential tunability, but still yield electron-transfer

rates lower than the diffusional rates of substrates and have unproven long-term stability.

Conversely, controlled immobilization of enzymes at surfaces to enable high-rate direct electron transfer would eliminate the need for the mediator component and possibly lead to enhanced stability. Novel surface chemistries are required that allow protein immobilization with controlled orientation, such that a majority of active centers are within electron-tunneling distance of the surface. Additionally, spreading of enzymes on the surfaces must be minimized to prevent deactivation due to irreversible changes in secondary structure. Finally, structures of controlled nanoporosity must be developed to achieve such surface immobilization at high volumetric enzyme loadings.

Along with electronic transport improvements must come attention to substrate transport in such porous structures. As discussed above, introduction of gas-phase diffusion or liquid-phase convection of reactants is a feasible approach to enabling high-current-density operation in electrodes of thicknesses exceeding 100 μm. Such a solution is application specific, in the sense that neither gas-phase reactants nor convection can be introduced in a subclass of applications, such as devices implanted in human, animal, or plant tissue. In the context of physiologically implanted devices, the choice becomes either milliwatt to watt scale devices implanted in a blood vessel, where velocities of up to 10 cm/s can be present, or microwatt-scale devices implanted in tissue. Ex vivo applications are more flexible, partially because gas-phase oxygen from ambient air will almost always be utilized on the cathode side, but also because pumps can be used to provide convective flow of any substrate. However, power requirements for pump operation must be minimized to prevent substantial lowering of net power output.[170]

Perhaps most importantly, the issue of system lifetime must be addressed. The electrodes and systems described above have demonstrated lifetimes ranging from days to months, depending greatly on the operating conditions and components involved. For a narrow range of applications, specifically week-long hospital stays or military missions, such lifetimes might be acceptable. However, for application in consumer devices or in surgically intensive implanted applications, system lifetime must be extended to the order of years. This is no simple prescription, owing not only to the limited lifetime of redox enzymes themselves but also to the limited chemical and mechanical stability of other electrode components, primarily electron mediators.[9,10,101,107]

Stabilization of activated oxidoreductases on time scales of months to years has historically been challenging, and the lack of success in this regard has limited the industrial implementation of redox enzymes to applications that do not require long lifetimes. However, as mentioned in the Introduction, some possibility of improved stability has arisen from immobilization of enzymes in hydrophilic cages formed by silica sol−gels and aerogels, primarily for sensor applications.[178−181] The tradeoff of this approach is expected to be a lowering of current density because of mass-transfer limitations. Such a tradeoff can be avoided to a certain extent by clever design of high-porosity aerogels with pore sizes ranging from nanoscale to micron scale, but ultimately a balance must be struck between activity and stability.

Having designed the respective cathode and anode with the required power density for a particular application, the final step involves the integration of a biofuel cell with electrical devices. Major integration issues include electrical integration (packaging and voltage matching), fuel delivery, waste removal, and safety. Multicell stacks are desirable to produce the conventional 1−5 V output voltage. Depending on the cell design, whether disposable or rechargeable, a nonambient fuel supply must be either integrated within the cell body or provided as replaceable cartridges. In disposable biofuel cells, environmental constraints and material recycling must be considered. Reaction products must be removed continuously, without any inhibitory or toxic effect on the biocatalyst. Overall safety features of the system, such as leakage or gas buildup, must be thoroughly addressed for both operational and storage conditions.

For biocatalysis to move forward as a viable means of catalyzing fuel cell reactions, the concerted efforts of biologists, chemists, chemical engineers, and materials scientists will be required. Niche applications in microwatt-scale implantable power might be accessible now, and the range of applications is expected to grow as the technology matures and energy demands expand. In the future, improved understanding of biocatalytic function, electron transfer, and substrate interactions will further the effort to put biological catalysts to work for electrical energy production.

7. Acknowledgment

S.C.B. and J.G. gratefully acknowledge the National Science Foundation for support under Award CTS-0239013.

8. References

(1) Yahiro, A. T.; Lee, S. M.; Kimble, D. O. *Biochim. Biophys. Acta* **1964**, *88*, 375.
(2) Drake, R. F.; Kusserow, B. K.; Messinger, S.; Matsuda, S. *Trans. Am. Soc. Artif. Intern. Organs* **1970**, *16*, 199.
(3) Davis, G.; Hill, H. A. O.; Aston, W. J.; Higgins, I. J.; Turner, A. P. F. *Enzyme Microb. Technol.* **1983**, *5*, 383.
(4) Grove, W. R. *Philos. Mag. J. Sci.* **1842**, *21*, 417.
(5) Gill, I. *Chem. Mater.* **2001**, *13*, 3404.
(6) Jin, W.; Brennan, J. D. *Anal. Chim. Acta* **2002**, *461*, 1.
(7) Gershenson, A.; Arnold, F. H. *Genet. Eng.* **2000**, *22*, 55.
(8) Binyamin, G.; Heller, A. *J. Electrochem. Soc.* **1999**, *146*, 2965.
(9) Binyamin, G.; Cole, J.; Heller, A. *J. Electrochem. Soc.* **2000**, *147*, 2780.
(10) Calabrese Barton, S.; Kim, H.-H.; Binyamin, G.; Zhang, Y.; Heller, A. *J. Phys. Chem. B* **2001**, *105*, 11917.
(11) Palmore, G. T. R.; Whitesides, G. M. *ACS Symp. Ser.* **1994**, *566*, 271.
(12) Katz, E.; Shipway, A. N.; Willner, I. In *Handbook of Fuel Cells—Fundamentals, Technology and Applications*; Vielstich, W., Gasteiger, H. A., Lamm, A., Eds.; John Wiley and Sons, Ltd.: London, 2003; Vol. 1, p 355.
(13) Heller, A. *Phys. Chem. Chem. Phys.* **2004**, *6*, 209.
(14) Reimers, C. E.; Tender, L. M.; Fertig, S.; Wang, W. *Environ. Sci. Technol.* **2001**, *35*, 192.
(15) Brodd, R. J. *Electrochem. Soc. Interface* **1999**, *8*, 20.
(16) Holmes, C. F. *Electrochem. Soc. Interface* **2003**, *12*, 26.

(17) Linden, D.; Reddy, T. B. *Handbook of Batteries*, 3rd ed.; McGraw-Hill: New York, 2002.
(18) Bhadra, N.; Kilgore, K. L.; Peckham, P. H. *Med. Eng. Phys.* **2001**, *23*, 19.
(19) Popovic, M. R.; Curt, A.; Keller, T.; Dietz, V. *Spinal Cord* **2001**, *39*, 403.
(20) Craelius, W. *Science* **2002**, *295*, 1018.
(21) Peckham, P. H.; Kilgore, K. L.; Keith, M. W.; Bryden, A. M.; Bhadra, N.; Montague, F. W. *J. Hand Surg.* **2002**, *27*, 265.
(22) Maynard, E. M. *Annu. Rev. Biomed. Eng.* **2001**, *3*, 145.
(23) Rauschecker, J. P.; Shannon, R. V. *Science* **2002**, *295*, 1025.
(24) Zrenner, E. *Science* **2002**, *295*, 1022.
(25) Tinoco, R.; Pickard, M. A.; Vazquez-Duhalt, R. *Lett. Appl. Microbiol.* **2001**, *32*, 331.
(26) Calabrese Barton, S.; Pickard, M.; Vazquez-Duhalt, R.; Heller, A. *Biosens. Bioelectron.* **2002**, *17*, 1071.
(27) Binyamin, G.; Chen, T.; Heller, A. *J. Electroanal. Chem.* **2001**, *500*, 604.
(28) Quinn, C. P.; Pathak, C. P.; Heller, A.; Hubbell, J. A. *Biomaterials* **1995**, *16*, 389.
(29) Quinn, C. A. P.; Connor, R. E.; Heller, A. *Biomaterials* **1998**, *18*, 11665.
(30) For current density, $i = nFDCd^{-1}Sh_{avg}^{-1}$, with $n = 2$, $F =$ Faraday's constant, glucose diffusion coefficient $D = 6.7 \times 10^{-7}$ cm^2/s, glucose bulk concentration $C = 5$ mM, and blood vessel diameter $d = 0.4$ cm. The average Sherwood number is given by $Sh_{avg} = 1.6(d^2vL^{-1}D^{-1})^{1/3}$, with average flow velocity v (cm/s) and electrode length $L = 1$ cm assumed.
(31) For spherical diffusion, $i = 2nFDC/d$, with parameters as defined in ref 30 and electrode diameter $d = 10$ μm.
(32) Agency Response Letter, GRAS Notice No. GRN 000122; U. S. Food and Drug Administration: Washington, DC, 2003; http://www.cfsan.fda.gov/~rdb/opa-g122.html (accessed July 2004).
(33) Agency Response Letter, GRAS Notice No. GRN 000106; U. S. Food and Drug Administration: Washington, DC, 2002; http://www.cfsan.fda.gov/~rdb/opa-g106.html (accessed July 2004).
(34) Bessant, R.; Steuer, A.; Rigby, S.; Gumpel, M. *Rheumatology* **2003**, *42*, 1036.
(35) Ayral, X. *Haemophilia* **2001**, *7*, 20.
(36) Shott, I. *Chem. Eng. News* **2003**, *81*, 146.
(37) Koelling, M. R.; Heiligmann, R. B. *North American Maple Syrup Producers Manual*; Ohio State University Extension: Columbus, OH, 1996.
(38) Rodriguez-Saona, L. E.; Fry, F. S.; McLaughlin, M. A.; Calvey, E. M. *Carbohydr. Res.* **2001**, *336*, 63.
(39) Prodolliet, J.; Hischenhuber, C. *Z Lebensm. Unters. Forsch. A: Food Res. Technol.* **1998**, *207*, 1.
(40) *AIJN Code of Practice for Evaluation of Fruit and Vegetable Juices*; Association of the Industry of Juices and Nectars from Fruits and Vegetables of the European Union: Brussels, Belgium, 1996.
(41) Markovarga, G. *J. Chromatogr.* **1987**, *408*, 157.
(42) Liden, H.; Volc, J.; Marko-Varga, G.; Gorton, L. *Electroanalysis* **1998**, *10*, 223.
(43) Ruzgas, T.; Csoregi, E.; Emneus, J.; Gorton, L.; MarkoVarga, G. *Anal. Chim. Acta* **1996**, *330*, 123.
(44) Tessema, M.; Csoregi, E.; Ruzgas, T.; Kenausis, G.; Solomon, T.; Gorton, L. *Anal. Chem.* **1997**, *69*, 4039.
(45) Ikeda, T.; Shibata, T.; Senda, M. *J. Electroanal. Chem.* **1989**, *261*, 351.
(46) Nilsson, G. S.; Andersson, M.; Ruzgas, T.; Garton, L. *Anal. Biochem.* **1998**, *265*, 151.
(47) Volponi, J. V.; Simmons, B. A.; Walker, A.; Ingersoll, D. *The Electrochemical Society Extended Abstracts*; The Electrochemical Society: Pennington, NJ, 2004; p 673.
(48) Akers, N. L.; Moore, C. M.; Minteer, S. D. *Electrochim. Acta* **2004**, in press.
(49) Akers, N. L.; Minteer, S. D. In *Fuel Cell Science, Engineering and Technology*; Shah, R. K., Kandlikar, S. G., Eds.; American Society of Mechanical Engineers: New York, 2004; p 497.
(50) Ren, X. M.; Zelenay, P.; Thomas, S.; Davey, J.; Gottesfeld, S. *J. Power Sources* **2000**, *86*, 111.
(51) Bittins-Cattaneo, B.; Wasmus, S.; Lopez-Mishima, B.; Vielstich, W. *J. Appl. Electrochem.* **1993**, *23*, 625.
(52) Sun, G. Q.; Wang, J. T.; Savinell, R. F. *J. Appl. Electrochem.* **1998**, *28*, 1087.
(53) Gupta, S.; Tryk, D.; Zecevic, S. K.; Aldred, W.; Guo, D.; Savinell, R. F. *J. Appl. Electrochem.* **1998**, *28*, 673.
(54) Vante, N. A.; Jaegermann, W.; Tributsch, H.; Hoenle, W.; Yvon, K. *J. Am. Chem. Soc.* **1987**, *109*, 3251.
(55) Reeve, R. W.; Christensen, P. A.; Hamnett, A.; Haydock, S. A.; Roy, S. C. *J. Electrochem. Soc.* **1998**, *145*, 3463.
(56) Borgwardt, R. H. *Transp. Res. D* **2001**, *6*, 199.
(57) Thurston, C. F.; Bennetto, H. P.; Delaney, G. M.; Mason, J. R.; Roller, S. D.; Stirling, J. L. *J. Gen. Microbiol.* **1985**, *131*, 1393.
(58) Suzuki, S.; Karube, I.; Matsunaga, T.; Kuriyama, S.; Suzuki, N.; Shirogami, T.; Takamura, T. *Biochimie* **1980**, *62*, 353.
(59) Karube, I.; Matsunaga, T.; Mitsuda, S.; Suzuki, S. *Biotechnol. Bioeng.* **1977**, *19*, 1535.
(60) Karube, I.; Suzuki, S.; Matsunaga, T.; Kuriyama, S. *Ann. N. Y. Acad. Sci.* **1981**, 91.
(61) Tanisho, S.; Kamiya, N.; Wakao, N. *Bioelectrochem. Bioenerg.* **1989**, *21*, 25.
(62) Ardeleanu, I.; Margineanu, D.-G.; Vais, H. *Bioelectrochem. Bioenerg.* **1983**, *11*, 273.
(63) Park, D. H.; Zeikus, J. G. *Appl. Environ. Microbiol.* **2000**, *66*, 1292.
(64) Kim, N.; Choi, Y.; Jung, S.; Kim, S. *Biotechnol. Bioeng.* **2000**, *70*, 109.
(65) Park, D. H.; Kim, S. K.; Shin, I. H.; Jeong, Y. J. *Biotechnol. Lett.* **2000**, *22*, 1301.
(66) Tsujimura, S.; Wadano, A.; Kano, K.; Ikeda, T. *Enzyme Microb. Technol.* **2001**, *29*, 225.
(67) Zhu, B.; Bai, X. Y.; Chen, G. X.; Yi, W. M.; Bursell, M. *Int. J. Energy Res.* **2002**, *26*, 57.
(68) Wilkinson, S. *Auton. Robots* **2000**, *9*, 99.
(69) Chaudhuri, S. K.; Lovley, D. R. *Nat. Biotechnol.* **2003**, *21*, 1229.
(70) Armstrong, F. A.; Hill, H. A. O.; Walton, N. J. *Q. Rev. Biophys.* **1985**, *18*, 261.
(71) Willner, I.; Katz, E. *Angew. Chem., Int. Ed.* **2000**, *39*, 1181.
(72) Pardo-Yissar, V.; Katz, E.; Willner, I.; Kotlyar, A. B.; Sanders, C.; Lill, H. *Faraday Discuss.* **2000**, 356.
(73) Willmer, I. *Acta Polym.* **1998**, *49*, 652.
(74) Kano, K.; Ikeda, T. *Anal. Sci.* **2000**, *16*, 1013.
(75) Ikeda, T.; Kano, K. *J. Biosci. Bioeng.* **2001**, *92*, 9.
(76) Willner, I.; Willner, B. *Trends Biotechnol.* **2001**, *19*, 222.
(77) Habermuller, K.; Mosbach, M.; Schuhmann, W. *Fresenius J. Anal. Chem.* **2000**, *366*, 560.
(78) Palmisano, F.; Zambonin, P. G.; Centonze, D. *Fresenius J. Anal. Chem.* **2000**, *366*, 586.
(79) Ghindilis, A. L.; Atanasov, P.; Wilkins, E. *Electroanalysis* **1997**, *9*, 661.
(80) Bartlett, P. N.; Tebbutt, P.; Whitaker, R. G. *Prog. React. Kinet.* **1991**, *16*, 55.
(81) Tarasevich, M. R. In *Comprehensive Treatise of Electrochemistry*; Srinivasan, S., Chizmadzhev, Y. A., Bockris, J. O. M., Conway, B. E., Yeager, E., Eds.; Plenum Press: New York, 1985; Vol. 10, p 231.
(82) Palmore, G. T. R.; Bertschy, H.; Bergens, S. H.; Whitesides, G. M. *J. Electroanal. Chem.* **1998**, *443*, 155.
(83) Tsujimura, S.; Fujita, M.; Tatsumi, H.; Kano, K.; Ikeda, T. *Phys. Chem. Chem. Phys.* **2001**, *3*, 1331.
(84) Pizzariello, A.; Stred'ansky, M.; Miertus, S. *Bioelectrochemistry* **2002**, *56*, 99.
(85) Bartlett, P. N.; Pratt, K. F. E. *J. Electroanal. Chem.* **1995**, *397*, 61.
(86) Hill, H. A. O. *Pure Appl. Chem.* **1987**, *59*, 743.
(87) Nakamura, K.; Aizawa, M.; Miyawaki, O. *Electro-enzymology, Coenzyme Regeneration*; Springer-Verlag: Berlin, 1988.
(88) Guo, L. H.; Hill, H. A. O. *Adv. Inorg. Chem.* **1991**, *36*, 341.
(89) Lotzbeyer, T.; Schuhmann, W.; Schmidt, H. L. *Sens. Actuators B: Chem.* **1996**, *33*, 50.
(90) Varfolomeev, S. D.; Kurochkin, I. N.; Yaropolov, A. I. *Biosens. Bioelectron.* **1996**, *11*, 863.
(91) Gorton, L.; Lindgren, A.; Larsson, T.; Munteanu, F. D.; Ruzgas, T.; Gazaryan, I. *Anal. Chim. Acta* **1999**, *400*, 91.
(92) Solomon, E. I.; Sundaram, U. M.; Machonkin, T. E. *Chem. Rev.* **1996**, *96*, 2563.
(93) Gupta, G.; Rajendran, V.; Atanassov, P. *Electroanalysis* **2004**, *16*, 1182.
(94) Tantillo, D.; Chen, J.; Houk, K. *Curr. Opin. Chem. Biol.* **1998**, *2*, 743.
(95) Sykes, A. G. *Adv. Inorg. Chem.* **1991**, *36*, 377.
(96) Cole, J. L.; Avigliano, L.; Morpurgo, L.; Solomon, E. I. *J. Am. Chem. Soc.* **1991**, *113*, 9080.
(97) Yamanaka, S.; Okawa, H.; Motoda, K.; Yonemura, M.; Fenton, D. E.; Ebadi, M.; Lever, A. B. P. *Inorg. Chem.* **1999**, *38*, 1825.
(98) Palmer, A. E.; Randall, D. W.; Xu, F.; Solomon, E. I. *J. Am. Chem. Soc.* **1999**, *121*, 7138.
(99) Palmer, A. E.; Lee, S. K.; Solomon, E. I. *J. Am. Chem. Soc.* **2001**, *123*, 6591.
(100) Mano, N.; Kim, H.-H.; Heller, A. *J. Phys. Chem. B* **2002**, *106*, 8842.
(101) Tsujimura, S.; Tatsumi, B.; Ogawa, J.; Shimizu, S.; Kano, K.; Ikeda, T. *J. Electroanal. Chem.* **2001**, *496*, 69.
(102) Machonkin, T. E.; Solomon, E. I. *J. Am. Chem. Soc.* **2000**, *122*, 12547.
(103) Calabrese, L. In *Electronics and Biotechnology Advanced (ELBA) Forum Series*; Nicolini, C., Ed.; Plenum Press: New York, 1998; Vol. 3, p 161.
(104) Musci, G.; Bellenchi, G. C.; Calabrese, L. *Eur. J. Biochem.* **1999**, *265*, 589.
(105) Farver, O.; Bendahl, L.; Skov, L. K.; Pecht, I. *J. Biol. Chem.* **1999**, *274*, 26135.
(106) Chen, T.; Calabrese Barton, S.; Binyamin, G.; Gao, Z.; Zhang, Y.; Kim, H.-H.; Heller, A. *J. Am. Chem. Soc.* **2001**, *123*, 8630.
(107) Palmore, G. T. R.; Kim, H.-H. *J. Electroanal. Chem.* **1999**, *464*, 110.

(108) Calabrese Barton, S.; Kim, H.-H.; Binyamin, G.; Zhang, Y.; Heller, A. *J. Am. Chem. Soc.* **2001**, *123*, 5802.
(109) Mano, N.; Kim, H. H.; Zhang, Y. C.; Heller, A. *J. Am. Chem. Soc.* **2002**, *124*, 6480.
(110) Kim, H. H.; Mano, N.; Zhang, X. C.; Heller, A. *J. Electrochem. Soc.* **2003**, *150*, A209.
(111) Moss, G. P. *Enzyme Nomenclature*; Nomenclature Committee of the International Union of Biochemistry and Molecular Biology (NC−IUBMB): London, 2003; http://www.chem.qmul.ac.uk/iubmb/enzyme/ (accessed Jul 2004).
(112) *Enzyme Nomenclature 1992*; Webb, E. C., Ed.; Academic Press: Orlando, FL, 1992.
(113) Blaedel, W. J.; Jenkins, R. A. *Anal. Chem.* **1975**, *47*, 1337.
(114) Fasman, G. D. *Practical Handbook of Biochemistry and Molecular Biology*; CRC Press: Boca Raton, FL, 1989.
(115) Chenault, H. K.; Whitesides, G. M. *Appl. Biochem. Biotechnol.* **1987**, *14*, 147.
(116) Gorton, L.; Dominguez, E. In *Encyclopedia of Electrochemistry*; Bard, A. J., Stratmann, M., Wilson, G. S., Eds.; Wiley: New York, 2002; Vol. 9, p 67.
(117) Simon, E.; Bartlett, P. N. *Surfactant Sci. Ser.* **2003**, *111*, 499.
(118) Scott, S. L.; Chen, W. J.; Bakac, A.; Espenson, J. H. *J. Phys. Chem.* **1993**, *97*, 6710.
(119) Karyakin, A. A.; Karyakina, E. E.; Schmidt, H. L. *Electroanalysis* **1999**, *11*, 149.
(120) Karyakin, A. A.; Karyakina, E. E.; Schuhmann, W.; Schmidt, H. L. *Electroanalysis* **1999**, *11*, 553.
(121) Willner, I.; Katz, E.; Patolsky, F.; Buckmann, A. F. *J. Chem. Soc., Perkin Trans. 2* **1998**, 1817.
(122) Willner, I.; Heleg-Shabtai, V.; Blonder, R.; Katz, E.; Tao, G.; Bueckmann, A. F.; Heller, A. *J. Am. Chem. Soc.* **1996**, *118*, 10321.
(123) Willner, I.; Arad, G.; Katz, E. *Bioelectrochem. Bioenerg.* **1998**, *44*, 209.
(124) Katz, E.; Riklin, A.; Heleg-Shabtai, V.; Willner, I.; Buckmann, A. F. *Anal. Chim. Acta* **1999**, *385*, 45.
(125) Katz, E.; Willner, I.; Kotlyar, A. B. *J. Electroanal. Chem.* **1999**, *479*, 64.
(126) Mao, F.; Mano, N.; Heller, A. *J. Am. Chem. Soc.* **2003**, *125*, 4951.
(127) Gao, Z.; Binyamin, G.; Kim, H.-H.; Calabrese Barton, S.; Zhang, Y.; Heller, A. *Angew. Chem., Int. Ed. Engl.* **2002**, *41*, 810.
(128) Riklin, A.; Katz, E.; Willner, I.; Stocker, A.; Buckmann, A. F. *Nature* **1995**, *376*, 672.
(129) Katz, E.; Heleg-Shabtai, V.; Willner, I.; Rau, H. K.; Haehnel, W. *Angew. Chem., Int. Ed.* **1998**, *37*, 3253.
(130) Forzani, E. S.; Otero, M.; Perez, M. A.; Teijelo, M. L.; Calvo, E. J. *Langmuir* **2002**, *18*, 4020.
(131) Pal, P.; Nandi, D.; Misra, T. N. *Thin Solid Films* **1994**, *239*, 138.
(132) Rajagopalan, R.; Heller, A. In *Molecular Electronics*; Aviram, A., Ratner, M., Eds.; New York Academy of Sciences: New York, 1997; p 241.
(133) Gregg, B. A.; Heller, A. *J. Phys. Chem.* **1991**, *95*, 5970.
(134) Daigle, F.; Trudeau, F.; Robinson, G.; Smyth, M. R.; Leech, D. *Biosens. Bioelectron.* **1998**, *13*, 417.
(135) Danilowicz, C.; Corton, E.; Battaglini, F. *J. Electroanal. Chem.* **1998**, *445*, 89.
(136) Blauch, D. N.; Saveant, J. M. *J. Am. Chem. Soc.* **1992**, *114*, 3323.
(137) Blauch, D. N.; Saveant, J. M. *J. Phys. Chem.* **1993**, *97*, 6444.
(138) Majda, M. In *Molecular Design of Electrode Surfaces*; Murray, R. W., Ed.; Wiley: New York, 1992; Vol. 22, p 159.
(139) Aoki, A.; Rajagopalan, R.; Heller, A. *J. Phys. Chem.* **1995**, *99*, 5102.
(140) Aoki, A.; Heller, A. *J. Phys. Chem.* **1993**, *97*, 11014.
(141) Zakeeruddin, S. M.; Fraser, D. M.; Nazeeruddin, M. K.; Gratzel, M. *J. Electroanal. Chem.* **1992**, *337*, 253.
(142) Lever, A. B. P. *Inorg. Chem.* **1990**, *29*, 1271.
(143) Buckingham, D. A.; Dwyer, F. P.; Sargeson, A. M. *Inorg. Chem.* **1966**, *5*, 1243.
(144) Buckingham, D. A.; Dwyer, F. P.; Sargeson, A. M. *Aust. J. Chem.* **1964**, *17*, 622.
(145) Forster, R. J.; Vos, J. G. *Macromolecules* **1990**, *23*, 4372.
(146) Degani, Y.; Heller, A. *J. Am. Chem. Soc.* **1989**, *111*, 2357.
(147) Cassidy, H. G.; Kun, K. A. *Oxidation−Reduction Polymers; Redox Polymers*; Interscience Publishers: New York, 1965.
(148) Murray, R. W. *Annu. Rev. Mater. Sci.* **1984**, *14*, 145.
(149) Heller, A. *Acc. Chem. Res.* **1990**, *23*, 128.
(150) Degani, Y.; Heller, A. *J. Phys. Chem.* **1987**, *91*, 1285.
(151) Degani, Y.; Heller, A. *J. Am. Chem. Soc.* **1988**, *110*, 2615.
(152) Degani, Y.; Heller, A. *J. Am. Chem. Soc.* **1989**, *111*, 2357.
(153) Pishko, M. V.; Katakis, I.; Lindquist, S. E.; Ye, L.; Gregg, B. A.; Heller, A. *Angew. Chem.* **1990**, *102*, 109.
(154) Trudeau, F.; Daigle, F.; Leech, D. *Anal. Chem.* **1997**, *69*, 882.
(155) Ohara, T. J.; Rajagopalan, R.; Heller, A. *Anal. Chem.* **1993**, *65*, 3512.
(156) Mano, N.; Mao, F.; Heller, A. *J. Am. Chem. Soc.* **2002**, *124*, 12962.
(157) Mano, N.; Kim, H. H.; Heller, A. *J. Phys. Chem. B* **2002**, *106*, 8842.
(158) Nakagawa, T.; Tsujimura, S.; Kano, K.; Ikeda, T. *Chem. Lett.* **2003**, *32*, 54.
(159) Tsujimura, S.; Kawaharada, M.; Nakagawa, T.; Kano, K.; Ikeda, T. *Electrochem. Commun.* **2003**, *5*, 138.
(160) Bard, A. J.; Faulkner, L. R. *Electrochemical Methods: Fundamentals and Applications*, 2nd ed.; John Wiley: New York, 2001.
(161) The mass-transfer boundary layer thickness, δ, on a rotating disk electrode can be estimated by $\delta = 1.6D^{1/3}\nu^{1/6}\omega^{-1/2}$, where D is the substrate diffusion coefficient, ν is the solution viscosity, and ω is the disk rotation speed.
(162) Campbell, C. N.; Heller, A.; Caruana, D. J.; Schmidtke, D. W. In *Electroanalytical Methods for Biological Materials*; Brajter-Toth, A., Chambers, J. Q., Eds.; Marcel Dekker: New York, 2002; p 439.
(163) Ianniello, R. M.; Lindsay, T. J.; Yacynych, A. M. *Anal. Chem.* **1982**, *54*, 1098.
(164) de Lumley-Woodyear, T.; Rocca, P.; Lindsay, J.; Dror, Y.; Freeman, A.; Heller, A. *Anal. Chem.* **1995**, *67*, 1332.
(165) Kenausis, G.; Taylor, C.; Katakis, I.; Heller, A. *J. Chem. Soc., Faraday Trans.* **1996**, *92*, 4131.
(166) Mano, N.; Heller, A. *J. Electrochem. Soc.* **2003**, *150*, A1136.
(167) Katz, E.; Filanovsky, B.; Willner, I. *New J. Chem.* **1999**, *23*, 481.
(168) Mano, N.; Mao, F.; Heller, A. *J. Am. Chem. Soc.* **2003**, *125*, 6588.
(169) Tsujimura, S.; Kano, K.; Ikeda, T. *Electrochemistry* **2002**, *70*, 940.
(170) Calabrese Barton, S. *Electrochim. Acta* **2003**, manuscript accepted.
(171) Newman, J. S. *Electrochemical Systems*, 2nd ed.; Prentice Hall: Englewood Cliffs, NJ, 1991.
(172) Giner, J.; Hunter, C. *J. Electrochem. Soc.* **1969**, *116*, 1124.
(173) Schroeder, P. *Z. Phys. Chem.* **1903**, *45*, 75.
(174) Boulatov, R. *Pure Appl. Chem.* **2004**, *76*, 303.
(175) Boulatov, R.; Collman, J. P.; Shiryaeva, I. M.; Sunderland, C. J. *J. Am. Chem. Soc.* **2002**, *124*, 11923.
(176) Bugg, T. D. H. *Tetrahedron* **2003**, *59*, 7075.
(177) Kim, E.; Chufan, E. E.; Kamaraj, K.; Karlin, K. D. *Chem. Rev.* **2004**, *104*, 1077.
(178) Chen, Q.; Kenausis, G. L.; Heller, A. *J. Am. Chem. Soc.* **1998**, *120*, 4582.
(179) Heller, J.; Heller, A. *J. Am. Chem. Soc.* **1998**, *120*, 4586.
(180) Lev, O.; Wu, Z.; Bharathi, S.; Glezer, V.; Modestov, A.; Gun, J.; Rabinovich, L.; Sampath, S. *Chem. Mater.* **1997**, *9*, 2354.
(181) Rabinovich, L.; Gun, J.; Tsionsky, M.; Lev, O. *J. Sol−Gel Sci. Technol.* **1997**, *8*, 1077.
(182) Sober, H. A. *CRC Handbook of Biochemistry: Selected Data for Molecular Biology*, 2nd ed.; CRC Press: Cleveland, OH, 1970.

CR020719K